Contents lists available at ScienceDirect

Deep-Sea Research Part I

journal homepage: www.elsevier.com/locate/dsri





Horizontal distribution of benthic and demersal fish assemblages on three seamounts in the Papahānaumokuākea Marine National Monument

Beatriz E. Mejía-Mercado¹, Amy R. Baco³

Department of Earth, Ocean and Atmospheric Science, Florida State University, EOAS Building, 1011 Academic Way, Tallahassee, FL, 32306, USA

ARTICLE INFO

Keywords:
Community structure
Seamounts
Northwestern Hawaiian islands
Horizontal distribution
Deep-sea fishes

ABSTRACT

Deep-sea fishes on seamounts have recently been shown to have strong changes in assemblage patterns with depth. However, horizontal variability patterns within a single seamount and among seamounts remain drastically understudied. The Papahānaumokuākea Marine National Monument (PMNM) is part of an extensive seamount chain that is relatively unimpacted by human activity as well as highly variable in physiographic and oceanographic characteristics. Three PMNM seamounts, Necker Island, French Frigate Shoals (FFS), and Pioneer Bank, were explored using Autonomous Underwater Vehicle surveys to document the deep-sea fish assemblages and their horizontal patterns of distribution at three different depths. Quantitative comparisons were made among the sides of the seamount and among the three seamounts while controlling for depth. The Gadiformes were the most abundant order with the highest number of individuals at 300 and 450 m on Pioneer and FFS. At 600 m the Myctophiformes showed the highest number of individuals overall and were the most abundant on FFS. Significant differences in abundance by seamount, side, and their interaction were observed at 300 and 600 m. Significant differences in some diversity metrics occurred in one, both, or the interaction of the factors of seamount and side at each depth. At all depths, the structure of the fish assemblage showed significant variation among seamounts and sides, which was explained mostly by the interaction term. After accounting for the variability explained by the confounding factor of time of day, the most common environmental factors related to assemblage structure for at least two depths were the east-west component of currents (u), latitude, chlorophyll a (chl a), and particulate organic carbon (POC). At 300 m, oxygen and salinity were also important, at 450 m mean direction of the substrate was an additional factor that was correlated with assemblage structure. At 600 m the factor that explained the most variation in community structure was percent rugosity. The results obtained in this study show significant horizontal variability in seamount fish assemblages within a given depth range; this variability should be taken into consideration in the management and conservation of the Monument and other seamounts.

1. Introduction

Deep-sea fishes are a critical element of benthic communities because they can control trophic structures while influencing the stability and resilience of other populations (Holmlund and Hammer, 1999). They can also migrate horizontally during different life stages, contributing to nutrient cycling by transporting and disseminating energy and nutrients from one place to another (Holmlund and Hammer, 1999). These roles make their characterization and distribution important to understand.

Patterns of distribution in deep-sea fishes have been widely studied

globally (Merrett and Haedrich, 1997; Rex and Etter, 2010). Vertically, benthic fish abundance is known to decrease with depth (Merrett and Haedrich, 1997; Rex and Etter, 2010), while species richness normally increases, peaks at different depths depending on the area, and then starts decreasing (Rex, 1981; Powell et al., 2003; Froese and Sampang, 2004; Priede et al., 2010). Horizontally, most studies have focused on continental margins where the highest species richness is generally found on the continental slope at a mean depth of 1500 m (Rex et al., 1993; Randall and Farrell, 1997).

On seamounts, several studies have also shown variability in vertical patterns of abundance and diversity (Parin, 1991; Parin et al., 1997;

E-mail address: abacotaylor@fsu.edu (A.R. Baco).

^{*} Corresponding author.

¹ Current address - Florida State University Coastal and Marine Laboratory, St. Teresa, Florida 32358, USA.

Tracey et al., 2004; McClain et al., 2010; Mejía-Mercado et al., 2019; Mejía-Mercado and Baco, 2022). Many of these studies have found depth to be an important correlate to the composition of fish assemblages, but at the same time, other depth-covariates such as temperature, salinity, and dissolved oxygen may be the important drivers (Snelgrove and Haedrich, 1985; Clark et al., 2010b, 2011; McClain et al., 2010; Mejía-Mercado et al., 2019).

Unlike depth patterns, horizontal variability in fishes inhabiting seamounts is less well understood. The two main studies that addressed horizontal variability on seamounts both were focused on South Pacific seamounts near New Zealand and used trawl gear as a sampling tool but did not control for depth in their comparisons. On a larger scale ($\sim\!1900$ km), Tracey et al. (2004) found that mean species richness was higher in New Zealand on the southern seamounts than on the northern seamounts. On a small spatial scale ($\sim\!9$ km), Tracey et al. (2012) found that fish abundance and species composition can vary between very close seamounts

Many gaps remain in our understanding of horizontal variation in fish fauna within and among seamounts. Seamounts have been demonstrated to be important refugia for deep-sea fishes (Rowden et al., 2010; Mejía-Mercado et al., 2019) and other benthic communities (Samadi et al., 2006; McClain et al., 2010), but the reality is that many seamounts around the world are being targeted by human activities such as fishing and mining (e.g., Clark et al., 2010b) that can decrease the abundance and diversity of seamount communities. A good location to gain a better understanding of horizontal variability in seamount fishes is the Papahānaumokuākea Marine National Monument (PMNM), which is a part of the Hawaiian-Emperor Seamount Chain and is situated in the northwestern portion of the Hawaiian Archipelago. The PMNM protects the banks, islands, and shoals, among other features that can be referred to as seamounts following the geological definition of Staudigel and Clague (2010), from mining and trawling. Only hook-and-line fishing for deepwater snappers and groupers has occurred on some of these seamounts (Haight et al., 1993). The remote location of the PMNM makes the Monument one of the few areas on Earth where investigation can be carried out without the influence of local human habitation and provides a unique opportunity to study seamounts in a relatively unimpacted state for comparison with other seamounts in heavily fished and exploited areas.

Besides protection, the PMNM also has great variability in oceanographic characteristics (Polovina et al., 1995; Firing and Brainard, 2006) that can influence the distribution of some benthic deep-sea fish assemblages facilitating horizontal larval dispersal (Koslow et al., 1994; Francis et al., 2002), or acting as a vertical barrier (Koslow et al., 1994) when interacting with the physiography of the area (Mundy, 2005). Among these factors, surface currents can be used to split the Hawaiian Archipelago into three sections. These sections loosely correspond to predicted breaks in connectivity based on biophysical modeling (Wren et al., 2016). The southeast portion, the geologically youngest area, consists of the Main Islands (outside of the Monument) and is influenced by the North Hawaiian Ridge Current (NHRC) that extends westward to just southwest of Necker Island (Qiu et al., 1997; Firing and Brainard, 2006) and at depths from near the surface to at least 200 m (Firing and Brainard, 2006; Desch et al., 2009). The middle portion of the Archipelago includes Necker Island and French Frigate Shoals among other underwater features and has the influence of the Subtropical Counter Current (STCC) flowing eastwards, but with some variation in the area depending on the season (Kobashi and Kawamura, 2002). Finally, the northwestern portion, the oldest seamounts, comprises mostly low atolls, banks, and sandy islets, including Pioneer Bank, where the mean currents flow northeast between Pearl and Hermes Atoll and Pioneer Bank (Firing, and Brainard, 2006).

Previous studies of the spatial distributions of deep-sea fishes in the Monument have shown vertical distribution patterns associated with depth and depth-related variables (Struhsaker, 1973; Chave and Mundy, 1994; Mejía-Mercado et al., 2019; Mejía-Mercado and Baco, 2022).

Significant variation with depth was observed in abundance, diversity of species, and the assemblage structure of fishes inhabiting seamounts. Three of these studies found evidence of different fish assemblages between depths of 200-700 m, with the deepest assemblage possibly related to the change in water masses in the area (Struhsaker, 1973; Mejía-Mercado et al., 2019; Mejía-Mercado and Baco, 2022). Using shrimp trawls, Struhsaker (1973) studied fish fauna in nine localities in the Hawaiian Islands at depths between 61 and 850 m. With most of the fish fauna being demersal (87.9%), the author observed that the fish composition was divided into four fish assemblages: 91-150 m, 151-250 m, 251-500 m, and 501-700 m. Mejía-Mercado et al. (2019) studied the fish fauna associated with the slopes of Necker Island from 250 to 700 m with an autonomous underwater vehicle (AUV). In this study fish assemblage composition changeover was observed at three depth ranges: 250-300 m, 350-500 m, and 550-700 m. Based on this fish assemblage changeover, Mejía-Mercado and Baco (2022) characterized the benthic and demersal fish fauna on Pioneer Bank, another seamount in the Monument, at 300, 450, and 600 m depths. These authors found that in terms of composition, there were at least two assemblages, one between 300 and 450 m and another at 600 m (Mejía-Mercado and Baco, 2022).

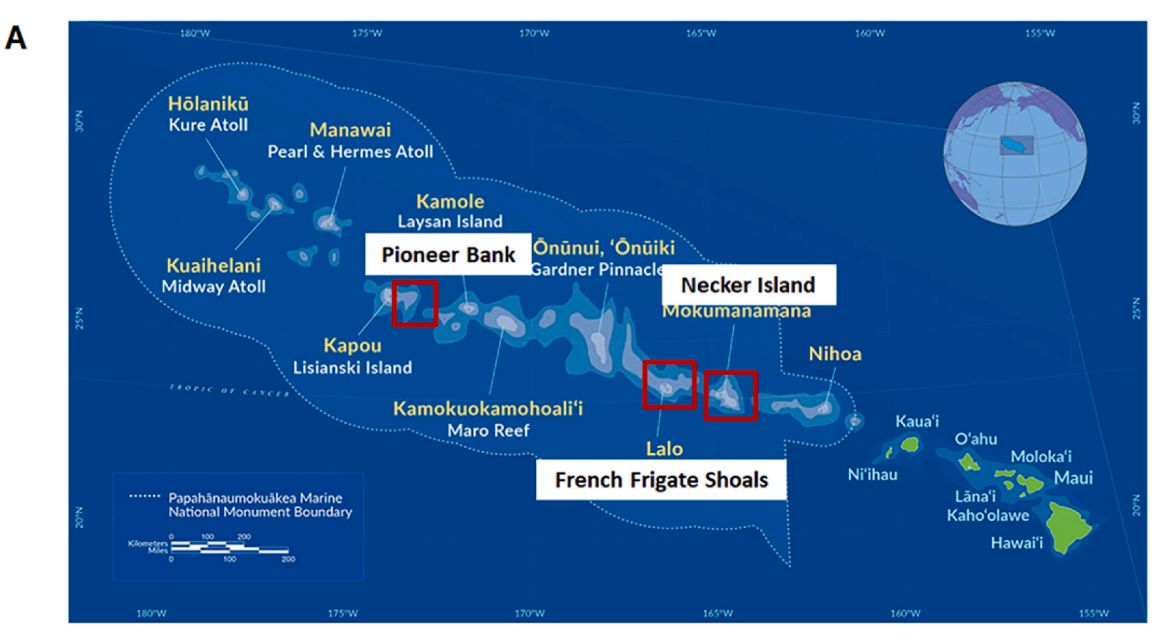
Horizontal distribution patterns of benthic and demersal fishes within a single seamount have also been studied recently in the Monument and have shown variability between sides of a single seamount within a given depth (Mejía-Mercado et al., 2019; Mejía-Mercado and Baco, 2022) over distances as small as ~75 km, as was observed on Necker Island (Mejía-Mercado et al., 2019). Given the level of variability within a single seamount, the next scale of horizontal variation to address then is variation among seamounts while controlling for depth. Questions that can be asked include whether the distance is a predictor of similarity among sites? Also, whether prevailing surface currents in the region influence similarity among seamounts on a given side? Relatedly, given the current patterns, would the fish assemblages on, for example, the north side of two different seamounts be more similar to each other than either side is to a different side on the same seamount? What environmental factors besides distance and currents are influencing the observed fish assemblage structure?

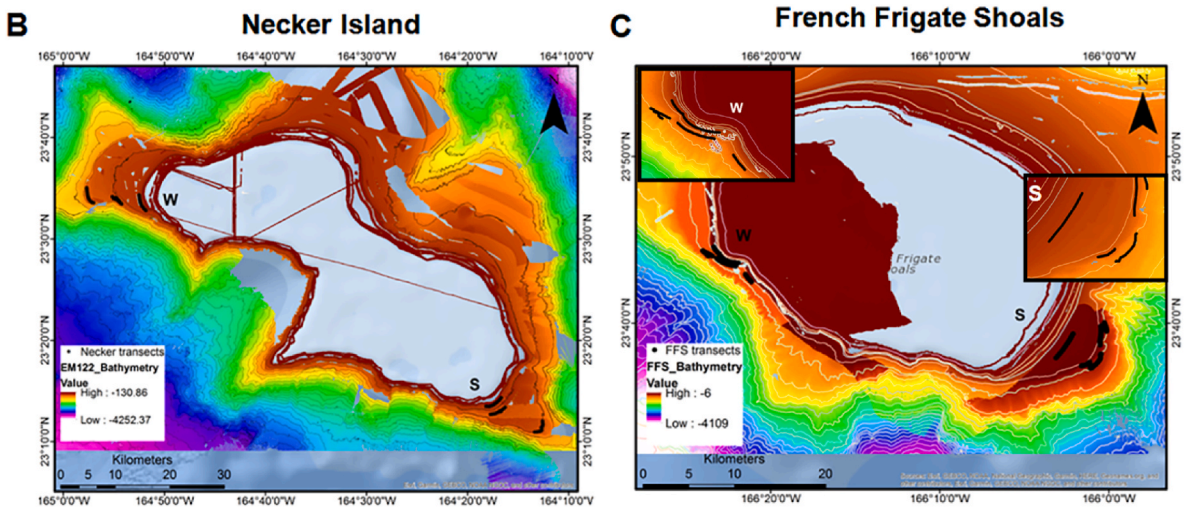
Considering the need to generate information about patterns of distribution that can be used to better understand seamount ecology and for management and conservation in the Monument and other areas, a quantitative study comparing the deep fish assemblages on the slopes around three PMNM seamounts was conducted. The three PMNM seamounts were Necker Island, a remnant volcanic cone with a summit 84 m above sea level, French Frigate Shoals, an atoll rising to 37 m above sea level, and Pioneer Bank with a flat summit 31 m below sea level. This study documents the benthic and demersal deep-sea fish assemblages and their horizontal patterns of distribution at three different depths. The objectives were to assess whether deep-sea fish assemblages change among seamounts at a given depth, to compare among seamount sides, and to determine which environmental variables are correlated with assemblage structure at each depth.

2. Materials and methods

2.1. Sampling locations

Three underwater features in a part of the Papahānaumokuākea Marine National Monument (PMNM) that has never been trawled, were targeted for this study; Necker Island, French Frigate Shoals, and Pioneer Bank (Fig. 1). These underwater features are considered seamounts based on the geomorphological definition (sensu Staudigel and Clague, 2010). Necker Island, located at 23°34′N-164°42′W, is a small volcanic island 150 m wide and <1200 m long (Macdonald et al., 1970) with its peak at 84 m above sea level (Evenhuis and Eldredge, 2004). Shallow water communities and ecosystems of this Island have been studied in the past (Parrish and Polovina, 1994; Weiss et al., 2009), while the





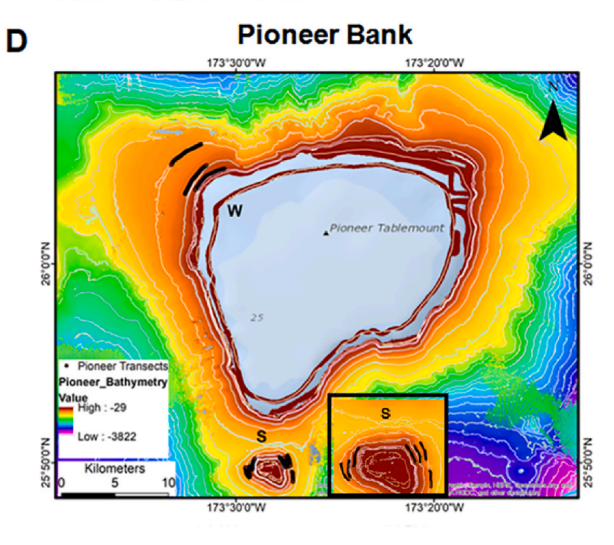


Fig. 1. A. Map of the Hawaiian Archipelago showing the Papahānaumokuākea Marine National Monument indicated by the white line and the sampled seamounts by the red boxes. B. Bathymetric maps of Necker Island (10 m and 70 m resolution), C. French Frigate Shoals (80 m resolution), and D. Pioneer Bank (40 m and 50 m resolution). AUV dive tracks are indicated by the thick black lines. Maps were created in ArcMap 10.4.1 (Esri, 2016). Both sides of FFF and one side of Pioneer Bank have inset zooms for better visualization.

extensive deeper slopes have just started to be studied (Mejía-Mercado et al., 2019; Morgan et al., 2019). French Frigate Shoals (FFS) is ca. 155 km from Necker Island at 23°45′N and 166°10′W. The shoals are the remaining part of an atoll and are 27 km in length (NOAA, 2003) with a well-developed barrier reef and lagoon (Kenyon et al., 2006). On FFS, La Perouse Pinnacles is the shallower part that rises 37 m above sea level (Grigg and Dollar 1980). The shallow ecosystems have been widely studied (e.g., DeMartini et al., 1996; DeMartini, 2004; Kenyon et al., 2006; Vroom et al., 2006), while the deeper ones have less information about their communities (e.g., Baco, 2007; Parrish and Baco, 2007). Pioneer Bank located at 26°00′N, 173°25′W, is a tablemount situated east of Lisianski Island and ca. 767 km from FFS. This bank measures approximately 29 km from northeast to southwest and close to 21 km from northwest to southeast, at its shallowest depth of 31.1 m (Uchida and Uchiyama, 1986). On this seamount, deep-sea studies have mainly

focused on the occurrence and distribution of fishes (e.g., Uchida and Uchiyama, 1986; Mundy, 2005); with recent work on the deep-sea fish community structure (Mejía-Mercado and Baco, 2022).

2.2. Data collection

Using the AUV Sentry (NDSF, 2019; https://ndsf.whoi.edu/sentry/) deployed from the RV Kilo Moana, Necker Island, French Frigate Shoals, and Pioneer Bank, were surveyed (Table 1, Fig. 1) as a part of a project examining the recovery potential of deep-sea coral communities impacted by trawling in the NWHI (Baco et al., 2019, 2020). Transects were located on the west and south sides of each seamount (Fig. 1B–D). Additional transects were taken on the NE side of Necker Island and Pioneer Bank (Mejía-Mercado et al., 2019; Mejía-Mercado and Baco, 2022), but weather prevented the survey of the third side on FFS, so only

Table 1
Location of AUV dives on Necker Island, French Frigate Shoals, and Pioneer Bank. On each side, 2–3 replicate transects of 1000 m length were conducted along depth contours at 300, 450, and 600 m. Complete information by transect is available in Table S1.

Seamount	Side	Transect Number	Latitude ^o N	Longitude ^o W	Depth (m)	Time of Sampling	Day/nigh
NKR	W	S360-07	23.572	164.874	300	18:44	night
		S360-08	23.562	164.870	300	19:11	night
		S360-09	23.553	164.863	300	19:39	night
		S360-18	23.568	164.907	450	0:52	night
		S360-19	23.564	164.904	450	1:33	night
		S360-20	23.569	164.912	450	2:01	night
		S360-30	23.565	164.950	600	7:27	day
		S360-31	23.574	164.958	600	7:57	day
		S360-32	23.584	164.960	600	8:26	day
	s	S361-06	23.226	164.293	300	20:34	night
		S361-07	23.231	164.285	300	21:04	night
		S361-08	23.239	164.278	300	21:36	night
		S361-16	23.223	164.271	450	2:37	night
		S361-17	23.217	164.278	450	3:11	night
		S361-18	23.214	164.286	450	3:45	night
		S361-32	23.201	164.209	600	11:44	day
		S361-33	23.191	164.210	600	12:09	day
		S361-34	23.184	164.213	600	12:33	day
FFS	W	S358-13	23.743	166.384	300	4:33	night
	••	S358-14	23.735	166.376	300	4:59	night
		S358-15	23.728	166.365	300	5:25	night
		S358-06	23.726	166.368	450	0:51	night
		S358-07	23.731	166.378	450	1:23	night
		S358-26	23.715	166.352	450	12:09	day
		S358-02 S358-03sd	23.739 23.738	166.394 166.391	600 600	22:16 22:51	night night
	<u> </u>	S359-07	·			6:18	
	3	S359-07 S359-08	23.656	166.035	300 300		day
			23.647	166.040		6:44	day
		S359-09	23.639	166.046	300	7:10	day
		S359-16	23.628	166.019	450	11:35	day
		S359-20	23.654	166.008	450	14:00	day
		S359-21	23.664	166.007	450	14:26	day
		S359-26	23.667	166.002	600	16:58	day
		S359-34	23.636	166.007	600	21:33	night
		S359-35	23.627	166.011	600	22:03	night
PION	W	S288-23	26.080	173.510	300	4:48	night
		S288-24	26.076	173.520	300	5:23	night
		S288-25	26.070	173.529	300	5:57	night
		S288-13	26.067	173.539	450	23:07	night
		S288-14	26.075	173.533	450	23:33	night
		S288-15	26.082	173.525	450	0:01	night
		S288-01	26.100	173.530	600	16:49	day
		S288-02	26.095	173.539	600	17:15	day
		S288-03	26.089	173.548	600	17:41	night
	s	S289-05	25.837	173.484	300	3:49	night
		S289-07	25.838	173.459	300	6:29	night
		S289-10	25.838	173.457	450	8:28	day
		S289-24s	25.830	173.488	450	1:23	night
		S289-01	25.829	173.489	600	23:15	night
							day
							day
		S289-13 S289-14	25.839 25.826	173.454 173.452	600 600	10:09 10:49	_

two sides of all three seamounts were analyzed in this study to maintain a balanced sample design. Both sides of Pioneer were surveyed in early December 2014. The transects at Necker and French Frigate Shoals were surveyed in late October and early November 2015. Video surveys were conducted during 24-h operations on each seamount, resulting in a difference in time of day among transects (Table 1). Between 2 and 3 replicate photo transects, of $\sim\!1000$ m in length, were taken on each side of each seamount along depth contours of 300, 450, and 600 m. The AUV speed was 0.5–0.7 m/s and its altitude from the bottom was between 3 and 8 m with an average of 5.5 m. The vehicle had a down-looking Allied Vision Technologies Prosilica GE4000C camera that allowed images with a resolution of 96 dpi (4008 \times 2672 pixels) and a field of view of about 12 m² to be taken every 3–4 s.

2.3. Taxonomic identification

This study was focused on benthic and demersal species. As defined by Randall and Farrell (1997), benthic species are "the species that are in physical contact with the bottom and are not very mobile" and demersal species are "the species that spend most of their lives near the bottom and move actively over the bottom". Following the same methodology applied in Mejía-Mercado et al. (2019) and Mejía-Mercado and Baco (2022), Sentry images were examined for the presence of benthic and demersal fishes on a 24-inch (60.96 cm) computer monitor. Because photos taken with the AUV overlapped, double counting fishes was avoided by recognizing the section of photos that overlapped and avoiding counting fishes in this section in the next photo(s). Also, the photos used for the identification of fishes were those with more than 80% seafloor visibility. Those photos with poor image quality (i.e. too high off the bottom or too close to the bottom, out of focus) were not analyzed. Observed fishes were taxonomically identified by B. Mejía--Mercado with a review by collaborator Bruce Mundy using Carpenter and Niem (1998, 1999a, 1999b, 2001a, 2001b), Chave and Malahoff (1998), Mundy (2005), Randall (2007), references cited in those publications, and unpublished notes on the identification of fishes in the Hawaiian biogeographic region gathered by collaborator Bruce Mundy. We followed Nelson et al. (2016) for the taxonomic classification of fishes and used a confidence score given to each photo identification on a scale of 1-4: (1) certainty in the species or genus, (2) certainty in the family, (3) certainty in the order, and (4) certainty in the class. All fishes counted were used to calculate relative abundance and for the descriptive statistics, these counts were standardized as the number of individuals divided by the number of photos. For the univariate and multivariate analyses, only counts of those organisms with a confidence score of 1 (genus and species level) were used and standardized by dividing by the number of photos as well. Each transect was 1000 m in length but there were slight variations in the number of useable photos because of terrain and image quality as noted above (Necker = 8483; FFS = 7245; Pioneer = 7836). Thus, to allow for comparison among transects, the fish counts were standardized by the number of useable photos in the transect.

2.4. Environmental data

A Kongsberg EM122 Multibeam Echosounder placed on the RV *Kilo Moana* and a Kongsberg EM302 Multibeam Echosounder placed on the RV *Sikuliaq* were used to acquire bathymetry and acoustic backscatter data for the three seamounts. The 10–20 m resolution data that was obtained did not cover the entire area surveyed, therefore, the bathymetries of the three seamounts were supplemented with data extracted online from NOAA (2019a, b, c): at 70 m resolution for Necker, 40–50 m for Pioneer and 80 m for FFS. With the sonar files cleaned in Qimera 3D editor, the raster grid files were obtained in Fledermaus (QPS software) and used to derive the contours using ArcGIS 10.4.1 (Esri, 2016). This information was then used to create the bathymetric maps of each seamount.

Each transect was mapped using XY layers in ArcGIS 10.0 obtained from the AUV ultra-short baseline tracking and the ship's Global Positioning System (GPS) tracking. The length of each transect was determined using the Geospatial Modeling Environmental package for R (Beyer, 2012). The aspect of the substrate, or direction the slope is facing, was computed from the sine and cosine layers created from the original aspect raster and the low-resolution bathymetries by using the Map Algebra function within ArcView (see Long and Baco, 2014) and then converted into mean direction of the substrate using the equations described by Fisher (1995).

In situ dissolved oxygen, temperature, conductivity, and depth were measured using an Aanderaa optode (model 4330) oxygen concentration sensor on the AUV Sentry and associated with each image at the time of image capture. Conductivity was converted into salinity using an algorithm in MATLAB described by Fofonoff and Millard (1983). For the W side of Pioneer, these variables were obtained from measurements made with a Seabird SBE49 Conductivity-Temperature-depth (CTD) that uses a Seapoint Optical Backscatter sensor. The reason for using these data was because on that side there were inconsistencies in the optode data that implied a malfunction during that dive.

Surface particulate organic carbon (POC), surface chlorophyll a (chl a), and surface current vectors were obtained from the study of Baco et al. (2017) as follows: POC and chl a were obtained from the National Oceanic and Atmospheric Administration's Environmental Research Division's Data Access Program (ERDDAP) Data Set (Simons, 2011). Monthly composites of POC and chl a extracted from the NESDIS satellite had a spatial resolution of 4 km. Surface chl a was also extracted from the Aqua-MODIS satellite with a spatial resolution of 0.025°. All data were extracted from January 2008 to December 2016. Daily values of surface current vectors u (east-west) and v (north-south) were extracted from HYCOM (Hybrid Coordinate Ocean Model), with a 1/12-degree spatial resolution, from January 1, 2015, to January 1, 2016, for all sides on all seamounts, except for the NW and S sides of the bank from which the data were extracted from January 1, 2014, to January 1, 2015. Quality control of all data (*. NetCDF) was made in Matlab and average values, which were used for the analyzes, were obtained in ArcMap 10.4.1 (Esri, 2016).

Substrate parameters, which included substrate composition, substrate size, rugosity, and slope, were determined for each transect following categorical scales (Table S2) as in Mejía-Mercado et al. (2019) and Mejía-Mercado and Baco (2022). Using every fourth photo, accomplishing 3-4 m coverage, substrate composition, and substrate size were determined using the point-count method with 15-random points as described in Mortensen and Buhl-Mortensen (2004), while rugosity and slope were estimated directly from the photo. For the analysis, substrate composition was summarized as the percentage (%) of sand from the total number of points in the transect. Substrate size was converted to a phi value following Mejía-Mercado and Baco (2022), in which the mean substrate for a transect was obtained and then multiplied by a phi value. The scale of the phi value described by Blair and McPherson (1999) was used with the addition of a phi value of -20for continuous hardpan substrate. Rugosity was expressed as the percentage of total images in each transect that did not show roughness (smooth surface), and slope as the percentage of total images in each transect that showed a slope of 0-50° (flat).

The time of day was converted into decimals of seconds by dividing the hours by 24 (24 h in a day), dividing the minutes by 60 (60 min in an hour), and then dividing the seconds by 3600 (3600 s in an hour). This variable was then made cyclical by transforming it into sine and cosine using the following formula for each transformation: Sine or Cosine (2 * pi * seconds/seconds in a day).

For the description of the environmental variables by seamount, daylight was considered as occurring from 6:00 a.m. to 5:30 p.m. for the sampled transects on Necker and FFS, and 6:30 a.m. to 5:30 p.m. for Pioneer, approximately half an hour before the sunrise and after the sunset time Hawaii (see https://sunrise-sunset.org/).

All environmental data collected on Necker Island, FFS, and Pioneer Bank for each transect at each study site can be found in the supplemental material (Table S1).

2.5. Statistical analyses

Necker and Pioneer were analyzed individually with a larger number of transects in Mejía-Mercado et al. (2019) and Mejía-Mercado and Baco (2022), respectively. Due to the fish assemblage changeover that was observed on Necker Island (Mejía-Mercado et al., 2019) and Pioneer Island (Mejía-Mercado and Baco, 2022), in the current study, subsets of transects from those studies were used in conjunction with transects from French Frigate Shoals (FFS) for comparisons among seamounts. The sampling effort for each depth was evaluated using species accumulation curves using the nonparametric estimators Chao 2, Jackknife 1, and Jackknife 2 to estimate the expected species richness. The curves were constructed with 10,000 randomizations (see Colwell and Coddington, 1994).

The deep-sea fish spatial variation was evaluated using standardized abundance (individuals/# photos), species richness (S), rarefaction estimates of the expected species richness in a 300-individual sample [E_S (300)], Shannon diversity (H', natural logarithms (nats)) and Simpson dominance (D) metrics. Because strong structuring by depth has been established for the NWHI seamounts (Long and Baco, 2014; Schlacher et al., 2014; Mejía-Mercado et al., 2019; Morgan et al., 2019; Mejía--Mercado and Baco, 2022), here the analyses were split into a separate set of analyses for each of the three depths of 300, 450, and 600 m. Each metric was then tested individually for each depth, without any treatment, using a two-way permutational analysis of variance (PERMA-NOVA) with crossed effects and fixed factors. The analysis of variance was constructed with Euclidean distance matrices, 10,000 permutations of residuals under a reduced model, and a sum of squares type III (partial model) and using Monte Carlo (MC) significance tests for the pairwise comparisons due to the low number of permutations (Anderson et al., 2008). The two fixed factors were Seamount (Necker, FFS, and Pioneer) and Side (W and S). Significant differences were tested using a p-value < 0.05. All statistical analyses and calculations of diversity indices were performed using PRIMER V6 + PERMANOVA software (Anderson et al.,

The deep-sea fish assemblage structure variation was assessed using a Permutational Multivariate Analysis of Variance (PERMANOVA), constructed with the fourth root transformed relative abundance data and the Bray-Curtis similarity matrix (Clarke and Warwick, 2001). The fourth root transformation (intermediate level) made it possible to reduce the contribution of very abundant species in relation to the less abundant without excluding the rarer species (Clarke and Warwick, 2001). Differences in assemblage structure by sides and seamounts were evaluated using the same permutational ANOVA design described above with a p-value $<\!0.05$.

Similarities in community structure among transects, by seamounts and sides, were visualized using Non-Metric Multidimensional Scaling (NMDS) ordinations and cluster analyses group average mode. Both analyses were based on the Bray-Curtis similarity matrix. SIMPROF analyses were used in the cluster analyses to test for any significant differences between clusters with a p < 0.05 and 10,000 residual permutations. Species contributions to the dissimilarity and similarity among the *a posteriori* groups obtained from the above analyses were determined using the Similarity Percentage Analysis (SIMPER) based on Bray-Curtis similarity matrices and with a 50% cut-off (Clarke and Warwick, 2001).

Variability of the environmental parameters among transects was explored for each depth using Principal Components Analysis (PCA). For this analysis that uses Euclidean distance, environmental variables were averaged by transect and normalized. Distance-based Linear Modeling (DistLM; Anderson et al., 2008) tests were performed to test for variables most strongly correlated with community structure by each depth. To

account for the potential confounding factors of time of day and spatial autocorrelation, a sequential DISTLM was used with a forward selection procedure and Akaike Information Criterion (AIC, Akaike, 1973) that allowed the model to choose which were the most important variables. A forward selection chooses one variable at a time, starting with the variable with the best value for the selection criterion and so on (Anderson et al., 2008). Spatial, temporal, and environmental variables at each depth were tested for high correlation and multicollinearity before performing DistLM analyses. A high correlation between two variables was determined by using draftsman plots with the normalized variables and a threshold of $r \ge +0.90$ or r < -0.90 (Clarke and Warwick, 2001), followed by the removal of one of each pair of correlated variables. Then, with the remaining variables, multicollinearity was tested using the Vegan package (Oksanen et al., 2010) in the R statistical program (R Development Core Team, 2018), by removing one variable at a time, starting with the one with the highest collinearity until only those variables with a variance inflation factor (VIF) less than five remained (Neter et al., 1996; Chatterjee et al., 2000; Zuur et al., 2010).

3. Results

3.1. Habitat description

Habitat characteristics were different by seamounts and by side on each seamount at each sampled depth (Table 1 and Table S1). At 300 m, Pioneer had the lowest average value of oxygen on the west side (6.72 mg/l) and the highest average value on the east side (7.99 mg/l). Temperature and salinity were the lowest on the south side of Necker (11.57 °C and 34.23, respectively) and the highest on the west side of Pioneer (13.48 °C and 34.42, respectively). Necker showed sandy substrates, with flat slope and very low rugosity; Pioneer and FFS showed harder substrates than Necker with flat slope and high rugosity, except for the south side of Pioneer and the south side of FFS that showed a steeper slope and low rugosity, respectively. POC was the lowest on the south side of Necker (31.85 mg/m3), and the highest on the west side of FFS (42.99 mg/m3). Based on satellite data, the W and S sides of FFS showed the highest average values of chl a (0.27 and 0.11 mg/m3, respectively). Current vector v was faster on both sides of Pioneer (0.08 m/s), but current vector u was slower on both sides of this seamount. Time of sampling on the W side of FFS and both sides of Necker and Pioneer was during the night; the S side of FFS was sampled during the day (Table 1).

At 450 m, FFS had the lowest average values of dissolved oxygen, temperature, and salinity on both sides compared to the other seamounts. The S side of Necker and the W side of FFS were the only ones with sandy substrates. The percentage of slope was similar on all sides of the three seamounts at 91-100% of a $0-50^{\circ}$ slope. Low rugosity was observed on the S side of Necker, and the W side of FFS and Necker. POC and chl a were the lowest on both sides of Necker and the highest on both sides of FFS. Current vector v showed the lowest values on FFS, while the highest value of current vector v was observed on the S side of FFS and the W side of Necker. The W side of FFS was sampled mostly during the night, while the SE was during the day. Both sides of Necker and the W side of Pioneer were sampled during the night. The S side of Pioneer had one transect sampled during the day and another during the night (Table 1).

At 600 m, values of dissolved oxygen, temperature, and salinity were similar on both sides of FFS and Necker and lower that the values measured on Pioneer. Sandy substrates were observed only on FFS. There was a high proportion of low slope on all sides on all seamounts, while low rugosity was observed mainly on the W side, except for Necker. POC and chl *a* were high on FFS, mostly on the S side. Current vector v was the lowest on both sides of FFS and the highest on the S side of FFS and the W side of Necker. Almost all transects on both sides of FFS were sampled during the night, except for one on the S side, whereas on both sides Necker all transects were conducted during the day. Both

sides of Pioneer had transects conducted during the day and the night (Table 1).

A PCA plot of environmental data for each transect at 300 m shows a clear separation between Pioneer and the other two seamounts along axis 1, which explains 38.5% of the variation (Fig. 2A). This axis was highly correlated with the current vector u (Fig. 2A). The three

seamounts separated along axis 2, which explained 25% of the variation and was most strongly correlated with chl *a*. At 450 m depth, there was a clear separation of transects between Pioneer and the other two seamounts along axis 1 (31.4% of variation). FFS was split with the S side grouping high on axis 2 (23.9% of variation) and the W side standing out from all other sites along both axes. Temperature was strongly

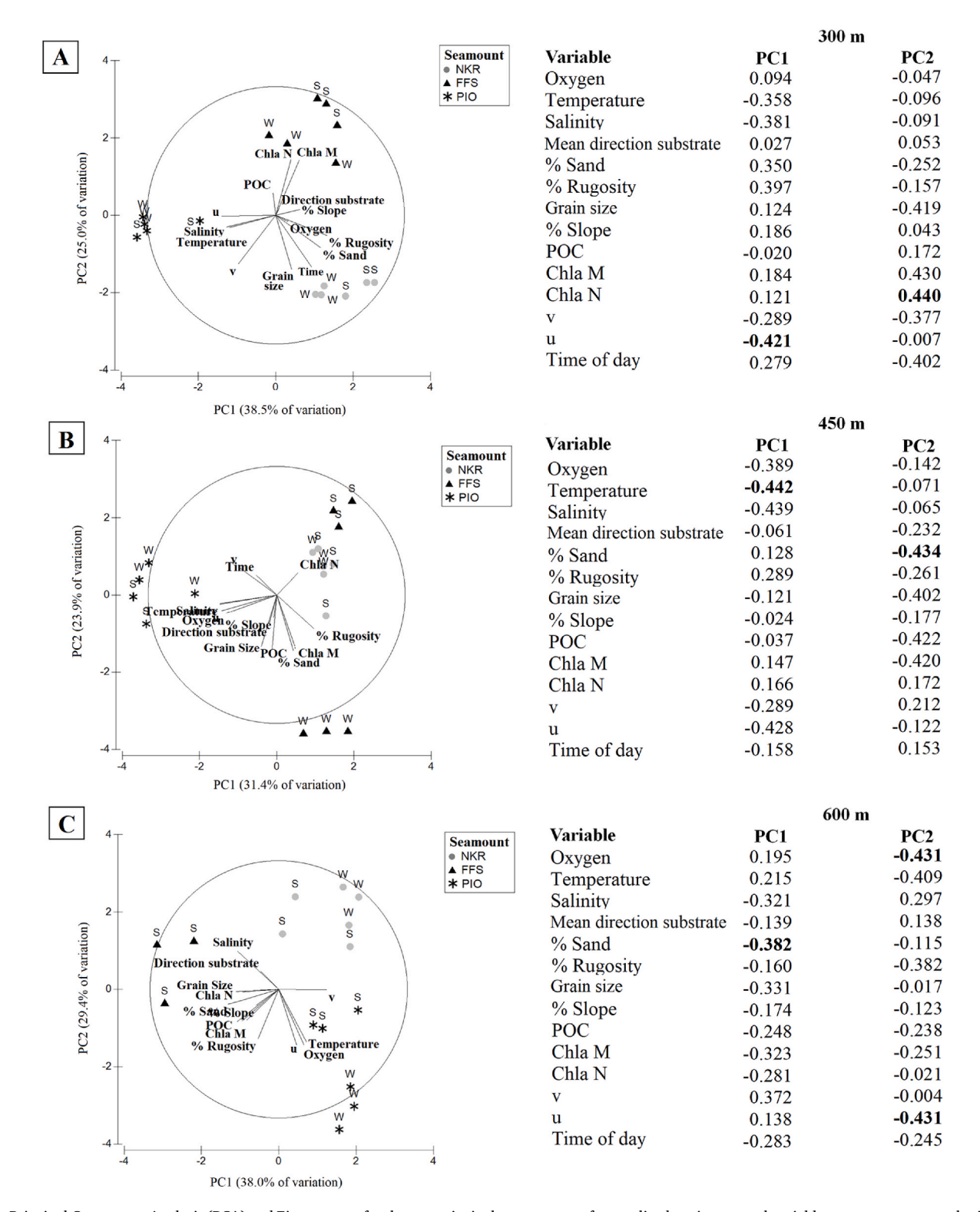


Fig. 2. Principal Component Analysis (PCA) and Eigenvectors for the two principal components of normalized environmental variables per transect were obtained on the three seamounts at A) 300, B) 450, and C) 600 m depth. Vectors show the direction and strength of each environmental variable relative to the overall distribution. Seamounts are indicated with symbols and sides are labeled for each transect. Bold values indicate the variables with the highest eigenvectors for each principal component.

correlated with axis 1 and % sand strongly correlated with axis 2 (Fig. 2B). At 600 m, a separation between FFS and the other two seamounts was observed along axis 1 that was highly correlated with % sand. Likewise, the W side of Pioneer and Necker separated strongly from all other sides on axis 2. This axis was most strongly correlated with oxygen and current vector u (Fig. 2C).

3.2. Descriptive analyses

The spatial variability of fish communities on Necker Island at depths from 250 to 700 m and on Pioneer Bank at depths of 300, 450, and 600 m was examined individually and discussed extensively in Mejía--Mercado et al. (2019) and Mejía-Mercado and Baco (2022), respectively. Results from a subset of the total transects in those studies are repeated briefly here for comparative purposes. Using all the organisms identified with the four confidence scores mentioned in the methodology and standardized by the number of photos, at 300 m across all seamounts, 68 species were identified in 40 families and 21 orders (Table 2). Eight of the 21 orders showed relative abundances over all transects above 5% with Gadiformes accounting for 27% of the overall total followed by Stomiiformes and Scorpaeniformes both with 14% (Fig. 3A). Gadiformes showed the highest relative abundance on the W side of Necker, both sides of Pioneer, and on the S side of FFS (Fig. 3A). The highest standardized abundance of Gadiformes was observed on Pioneer and the W side of FFS (Fig. 4A). The Stomiiformes showed the highest relative abundance on the S side of Necker and on the S side of Pioneer (Fig. 3A), where standardized abundance was also the highest (Fig. 4A). The Scorpaeniformes showed high relative abundance mainly on the W sides of Necker and Pioneer (Fig. 3A), while the standardized abundance was high on both sides of FFS and Pioneer (Fig. 4A). Gadiformes was very abundant because of the species Laemonema sp., but many organisms within this order were not able to be identified to the lowest taxonomic level. Stomiiformes was mainly represented, in terms of abundance, by only one species Argyripnus sp., and Scorpaeniformes by Bembradium roseum (Table 2).

At 450 m, 62 species were identified in 36 families and 19 orders (Table 2). Six of the 19 orders had relative abundances greater than 5% with Gadiformes accounting for 37% of the total population followed by Scorpaeniformes (18%) and Stomiiformes (16%) (Fig. 3B). The Gadiformes showed the highest relative abundance on the W sides of Necker, Pioneers, and FFS (Fig. 3B), while the standardized abundance was the highest on the W side of Pioneer (Fig. 4B). The Scorpaeniformes showed high relative abundance on the W side of FFS (Fig. 3B), but the standardized abundance was higher on the W side of Pioneer (Fig. 4B). The Stomiiformes showed the highest relative abundance, 82% of the individuals, on the S side of Necker (Fig. 3B), while the highest number of individuals per photo was observed on the W side of Pioneer (Fig. 4B). Beryciformes also showed notably high standardized abundance on the S side of FFS. Gadiformes was highly abundant due to the macrourids Malacocephalus cf. hawaiiensis and Coelorinchus gladius, and the morid Laemonema rhodochir. Scorpaeniformes are represented mainly by the three following species: Scorpaena pele, Scalicus engyceros, and Bembradium roseum. Stomiiformes was very abundant due to the species Argyripnus sp. (Table 2).

At 600 m, 54 species were identified in 31 families and 17 orders of deep-sea fishes (Table 2). Of these orders, only two showed abundances greater than 5%, the Myctophiformes, which accounted for 75% of the total population, and the Gadiformes for the remaining 25% (Fig. 3C). The Myctophiformes showed the highest relative abundance on the W sides of Necker and FFS (Fig. 3C), while its standardized abundance was the highest on the W side of FFS (Fig. 4C). The Gadiformes showed the highest relative abundance on the W side of Pioneer, and the S sides of Necker and FFS (Fig. 3C), but the standardized abundance was the highest on the W side of FFS (Fig. 4C). The high abundance of organisms within Myctophiformes was due to only one species, *Neoscopelus macrolepidotus*, whereas the high abundance of Gadiformes was mainly due

to the species Malacocephalus cf. hawaiiensis and Ventrifossa atherodon (Table 2).

3.3. Univariate analyses

According to the species accumulation curves that were performed using the organisms identified at the genus or species level (confidence score 1), 68 species identified at 300 m depth represented between 72 and 79% of the species richness expected for this depth. At 450 m, 62 species identified were between 67 and 74% of the species richness expected. At 600 m, 52 species identified represented between 75 and 83% of the species richness expected. At all depths, Jackknife 2 had the maximum expected richness, while Chao 2 had the minimum expected richness for 300 and 450 m, and Jackknife 1 had the minimum expected richness for 600 m (Fig. S1).

At 300 m, abundance showed a significant difference among seamounts, sides, and the interaction of both factors (p < 0.001, p = 0.009, and p < 0.001, respectively) (Table 3). The pairwise tests showed significant differences between FFS and the other two seamounts as well as between both sides of FFS. This seamount had the highest abundance with more individuals per transect on the W side (Fig. S2A). Species richness also showed a significant difference, but only in the interaction term (p = 0.011) (Table 3). According to the pairwise tests, the differences are between both sides on Necker and between Necker and FFS on the S side. The S side of Necker has the highest mean number of species compared to the other side of the island and the sides of the other seamounts (Fig. S2A). Shannon diversity, E_S (300), and Simpson Dominance were not significantly different among seamounts, sides, or the interaction (Table 3).

At 450 m, abundance only showed a significant difference among seamounts (P = 0.007) (Table 3). The pairwise tests showed differences between FFS and the other two seamounts, where FFS had the highest abundance among the seamounts (Fig. S2B). Species and $E_{S\ (300)}$ did not show significant differences by either factor or their interaction, but Shannon diversity and Simpson dominance showed significant differences by side (P = 0.013 and P = 0.012, respectively) (Table 3). The highest diversity and lowest dominance were observed on the W side of all seamounts (Fig. S2B).

At 600 m, abundance showed a significant difference among seamounts, sides, and their interaction (p = 0.014, p = 0.010, and p <0.001, respectively) (Table 3). The pairwise tests showed differences between FFS and the other two seamounts, with FFS having the highest abundance on its S side (Fig. S2C). Species richness showed significant differences among seamounts (p = 0.043), while $E_{S(300)}$ showed significant differences in the interaction of both factors (p = 0.012) (Table 3). The pairwise tests showed differences in species richness and E_S (300) between FFS and Pioneer, but they also showed low differences in E_{S (300)} between both sides of FFS. FFS had the highest species richness among seamounts, particularly on the S side (Fig. S2C). Shannon diversity and Simpson Dominance were significantly different among seamounts (p = 0.010 and p = 0.020, respectively) and the interaction (p = 0.009 and p = 0.005, respectively) (Table 3). Both attributes showed differences between FFS and the other two seamounts, as well as between FFS and the S side of Pioneer. FFS had the highest diversity with the lowest dominance on the S side, whereas the lowest diversity with high dominance was observed on the S side of Pioneer (Fig. S2C).

3.4. Multivariate analyses

The multivariate PERMANOVA tests showed significant differences in fish assemblage structure among seamounts, sides, and their interaction at each of the three depths (Table 4). At 300 m, the PERMANOVA model explained 78.6% of the variation and the most important factor in this variation was "seamount" (30.8%) (Table 4). The pairwise comparisons for the interaction showed that within a given side, there were differences among seamounts on both sides (W and S). Within a given

Table 2
Deep-sea fish composition and absolute abundance observed on two sides (W and S) of Necker Island, French Frigate Shoals, and Pioneer Bank arranged by depth. The total number of observations is shown in gray and data is shown by depth (300, 450, and 600 m). The taxonomic classification follows Nelson et al. (2016). The identification confidence scores (ICS) given to each taxonomic identification are presented as (1) total certainty in the species or genus identification, (2) certainty in the family identification, and (3) certainty in the order identification.

					Neck	er	Fre	nch Fr	igate		Pion	eer
				W	S	Total	\mathbf{W}	\mathbf{S}	Total	W	S	Total
	300 m											
Class Chondrichthyes												
Order	Family	Species	ICS									
Squaliformes	Centrophoridae	Centrophorus sp.	1		1	1				1	1	2
	Etmopteridae	Etmopterus pusillus	1		2	2	5		5			
	Squalidae	Squalus hawaiiensis	1	10	6	16	1	1	2	21		21
Class Osteichthyes												
Anguilliformes		Anguilliformes	3					1	1			
	Congridae	Ariosoma marginatum	1					1	1			
		Ariosoma sp.	1	2	2	4	20		20			
		Conger oligoporus	1	1		1		1	1			
		Gnathophis cf. heterognathos	1	22	17	39		4	4	30		30
		Gnathopis sp.	1				2		2			
	Nettastomatidae	Nettastoma parviceps	1	1	2	3	1	1	2	1		1
	Ophichthidae	Ophichthidae sp. 1	1		2	2	4	1	5			
		Ophichthus kunaloa	1		4	4	1		1			
		Ophichthidae	2								1	1
	Synaphobranchidae	Ilyophis sp. 1	1	1	3	4	2	4	6		1	1
		Ilyophis sp. 2	1					3	3			
		Meadia abyssalis	1				1		1			
		Synaphobranchidae sp. 2	1	1		1						
		Synaphobranchus sp. 1	1					1	1		1	1
Argentiniformes	Argentinidae	Glossanodon struhsakeri	1		3	3	3	6	9	1		1
Stomiiformes	Sternoptychidae	Argyripnus sp.	1		483	483	17		17	22	93	115
Ateleopodiformes	Ateleopodidae	Ijimaia plicatellus	1	1		1						
Aulopiformes	Ipnopidae	Ipnopidae	2	5		5						
	Chlorophthalmidae	Chlorophthalmus proridens	1		9	9						
	Synodontidae	Synodus kaianus	1	29	2	31	2	7	9			
Myctophiformes	Myctophidae	Myctophidae	2	7		7						
	Neoscopelidae	Neoscopelus macrolepidotus	1				84		84	13	1	14
Polymixiiformes	Polymixiidae	Polymixia nobilis	1				20	1	21	3	1	4
Gadiformes		Gadiformes	3	110		110	2	5	7	70	33	103
	Macrouridae	Coelorinchus gladius	1		4	4	10		10			
		Coelorinchus tokiensis	1				1		1			
		Malacocephalus cf. hawaiiensis	1				3		3		4	4
		Pseudocetonurus septifer	1		2	2						
		Ventrifossa atherodon	1							1		1
		Macrouridae	2	44	21	65	19	3	22	4	1	5
	Moridae	Laemonema rhodochir	1				1		1		1	1
		Laemonema sp.	1	8	46	54	25	27	52	3	18	21
		Physiculus grinnelli	1				1		1			
		Physiculus nigripinnis	1				3	3	6	3	10	13
		Moridae	2		10	10	4	5	9	14	28	42

Holocentriformes	Holocentridae	Pristilepis oligolepis	1								2	2
Trachichthyformes	Trachichthyidae	Hoplostethus crassispinus	1				1		1		3	3
Beryciformes	Berycidae	Beryx decadactylus	1								2	2
•	•	Beryx splendens	1				5		5	5	3	8
Ophidiiformes		Ophidiiformes	3	2	1	3						
•	Carapidae	Pyramodon ventralis	1	_	15	15	1	8	9	2	3	5
	Ophidiidae	Ophidiidae sp. 5	1		1	1	•	2	2	_		Ü
Carangiformes	Caragidae	Seriola dumerili	1		•	•		1	1			
	· ·	Ophidion muraenolepis	1		3	3	1	2	3	3		3
Pleuronectiformes	Bothidae	Bothidae sp. 1	1		-	_	1	3	4			_
		Bothidae sp. 2	1					2	2			
		Chascanopsetta crumenalis	1		3	3						
		Chascanopsetta prorigera	1	3	7	10		1	1	4		4
		Parabothus cf. coarctatus	1	28	7	35	27	10	37			
		Poecilopsetta hawaiiensis	1	7		7	1		1			
		Taeniopsetta radula	1	21	2	23						
		Bothidae	2	1		1		3	3			
	Cynoglossidae	Symphurus strictus	1		2	2						
Callionymiformes	Callionymidae	Synchiropus kinmiensis	1					3	3			
Scombriformes	Gempylidae	Rexea nakamurai	1				13		13	2	4	6
Trachiniformes	Percophidae	Chrionema chryseres	1		1	1	49	8	57	15	37	52
		Chrionema squamiceps	1	1		1	3	10	13	14		14
		Percophidae	2				15		15			
	Pinguipedidae	Parapercis roseoviridis	1				3		3			
Perciformes		Perciformes	3					2	2			
	Epigonidae	Epigonidae	2								1	1
	Lutjanidae	Etelis carbunculus	1								3	3
		Pristipomoides filamentosus	1	5		5	1		1			
	Serranidae	Plectranthias kelloggi	1				1		1			
	Symphysanodontidae	Symphysanodon maunaloae	1	1	43	44	47	18	65	2	4	6
Scorpaeniformes		Scorpaeniformes	3		2	2						
	Bembridae	Bembradium roseum	1		28	28	19	21	40	49	1	50
	Hoplichthyidae	Hoplichthys citrinus	1	10	4	14		2	2	1		1
	Peristediidae	Scalicus engyceros	1	73	1	74	1		1		1	1
		Scalicus hians	1	3		3						
	Scorpaenidae	Pontinus macrocephalus	1				2	2	4	1	10	11
		Scorpaena pele	1	1	5	6	5	2	7			
		Scorpaenidae sp. 6	1		1	1						
		Setarches guentheri	1		1	1	2		2		8	8
		Scorpaenidae	2							2	21	23
Lophiiformes		Lophiiformes	3							1		1
	Lophiidae	Lophiodes cf. bruchius	1							3		3
	Ogcocephalidae	Halieutaea retifera	1		1	1				1		1
		Malthopsis mitrigera	1	1	11	12				1		1

	450 m											
Class Chondrichthye	s											
Order	Family	Species	ICS									
Squaliformes	Centrophoridae	Centrophorus sp.	1					1	1	2		2
	Etmopteridae	Etmopterus pusillus	1					2	2			
	Squalidae	Squalus hawaiiensis	1	1	2	3	2	1	3	2		2
Class Osteichthyes												
Anguilliformes		Anguilliformes	3					1	1			
	Congridae	Ariosoma marginatum	1				1		1			
		Conger oligoporus	1		1	1		1	1			
		Gnathophis cf. heterognathos	1		1	1						
	Nettastomatidae	Nettastoma parviceps	1	2	1	3	1	1	2	2		2
	Ophichthidae	Ophichthidae sp. 1	1							1		1
		Ophichthus kunaloa	1	1		1						
	Synaphobranchidae	Ilyophis sp. 1	1	4	2	6	5	1	6	2	6	8
		Ilyophis sp. 2	1					4	4			
		Meadia abyssalis	1	1	1	2						
		Synaphobranchus sp. 1	1					4	4			
		Synaphobranchidae	2		3	3	1	1	2	2		2
Argentiniformes	Argentinidae	Glossanodon struhsakeri	1								7	7
Stomiiformes	Sternoptychidae	Argyripnus sp.	1	45	718	763	9	1	10	96		96
Aulopiformes	Chlorophthalmidae	Chlorophthalmus imperator	1	2		2						
		Chlorophthalmus proridens	1	7	36	43	7	1	8	21		21
Myctophiformes	Neoscopelidae	Neoscopelus macrolepidotus	1	19		19					2	2
		Neoscopelidae	2		4	4						
Polymixiiformes	Polymixiidae	Polymixia nobilis	1							37	5	42
Zeiformes	Grammicolepididae	Grammicolepis brachiusculus	1					2	2			
	Zeidae	Zenopsis nebulosa	1								1	1
	Zeniontidae	Cyttomimus stelgis	1	2	6	8	7	2	9	1	2	3
Gadiformes		Gadiformes	3	1		1		4	4	7	12	19
	Macrouridae	Coelorinchus aratrum	1	1		1						
		Coelorinchus gladius	1	8	7	15	14	1	15	70	4	74
		Coelorinchus tokiensis	1					1	1		2	2
		Hymenocephalus antraeus	1				7		7			
		Malacocephalus cf. hawaiiensis	1	35	22	57	20	16	36	66		66
		Pseudocetonurus septifer	1				1		1			
		Ventrifossa atherodon	1				2	1	3			
		Macrouridae	2	7		7	66	7	73	9		9
	Moridae	Laemonema rhodochir	1	28	27	55	30	53	53	9	12	21
		Laemonema sp.	1	15	23	38	1	1	2	5	3	8
		Physiculus grinnelli	1		1	1	Ů		Ĩ		5	Ü
		Moridae	2		8	8		14	14	8		8
Trachichthyiformes	Trachichthyidae	Hoplostethus crassispinus	1		2	2		17	17	U		U
Beryciformes	Berycidae	Beryx decadactylus	1		2	2	6	2	8		3	3
J -	· y -	Beryx splendens	1	2	9	11	U	140	140		3	5
		Berycidae Berycidae	2		J	11		140	140			

Ophidiiformes	Carapidae	Pyramodon ventralis	1	4		4	3	2	5			
Pleuronectiformes	Bothidae	Chascanopsetta prorigera	1	2	2	4	40	1	41	3		3
		Poecilopsetta hawaiiensis	1				1		1			
		Bothidae	2				3		3			
	Cynoglossidae	Symphurus strictus	1				3		3			
Scombriformes	Gempylidae	Rexea nakamurai	1				1		1			
		Ruvettus pretiosus	1					1	1			
Trachiniformes	Percophidae	Chrionema chryseres	1	17	40	57	33	19	52	12	39	51
		Chrionema squamiceps	1		2	2	6		6			
		Percophidae	2				1		1			
Perciformes	Lutjanidae	Pristipomoides filamentosus	1				3		3		7	7
	Epigonidae	Epigonus cf. glossodontus	1	3		3						
		Epigonus devaneyi	1		2	2						
		Epigonidae	2		1	1		5	5		18	18
	Pentacerotidae	Pentaceros wheeleri	1							1		1
	Symphysanodontidae	Symphysanodon maunaloae	1				4		4	39		39
Scorpaeniformes		Scorpaeniformes	3	5	1	6	4		4			
	Bembridae	Bembradium roseum	1	2	4	6	7	2	9	26	17	43
	Hoplichthyidae	Hoplichthys citrinus	1				2		2			
	Peristediidae	Scalicus engyceros	1		1	1	24		24	35	1	36
		Scalicus hians	1					1	1			
	Scorpaenidae	Scorpaena pele	1	2	1	3	29	6	35	26		26
		Scorpaenidae sp. 6	1	18	4	22	6		6	2		2
		Scorpaenidae sp. 7	1	9	4	13	2	5	7			
		Scorpaenidae sp. 8	1					1	1			
		Setarches guentheri	1	1		1		1	1			
		Scorpaenidae	2				6	2	8	2		2
Lophiiformes		Lophiiformes	3					1	1			
	Chaunacidae	Chaunax sp.	1					2	2	3		3
		Chaunax umbrinus	1		2	2		3	3	4	4	8
	Lophiidae	Lophiodes cf. bruchius	1		1	1						
	Ogcocephalidae	Malthopsis mitrigera	1		4	4				5		5
Tetraodontiformes	Triacanthodidae	Hollardia goslinei	1	2		2		1	1			

	600 m											
Class Chondrichthye	es											
Order	Family	Species	ICS									
Carcharhiniformes	Pseudotriakidae	Pseudotriakis microdon	1					1	1			
Squaliformes	Centrophoridae	Centrophorus sp.	1	1		1					1	1
	Etmopteridae	Etmopterus pusillus	1	2		2		2	2			
		Etmopteridae	2	1		1						
	Squalidae	Squalus hawaiiensis		1	2	3		1	1			
Class Osteichthyes												
Anguilliformes	Congridae	Ariosoma marginatum	1					1	1			
		Ariosoma sp.	1	7	2	9	6	6	12	1		1
	Nettastomatidae	Nettastoma parviceps	1	1		1		3	3	3	1	4
	Ophichthidae	Ophichthus kunaloa	1	1		1						
	Synaphobranchidae	Ilyophis sp. 1	1	7	7	14	1	2	3			
		Ilyophis sp. 2	1					2	2			
		Synaphobranchidae sp. 2	1	11		11						
		Synaphobranchidae	2				2		2			
Stomiiformes	Sternoptychidae	Argyripnus sp.	1					1	1			
Ateleopodiformes	Ateleopodidae	Ijimaia plicatellus	1				11		11	2		2
Aulopiformes	Chlorophthalmidae	Chlorophthalmus imperator	1		3	3						
		Chlorophthalmus proridens	1		15	15	18	6	24	74		74
		Chlorophthalmidae	2	5	4	9						
Myctophiformes	Neoscopelidae	Neoscopelus macrolepidotus	1	198		198	1439		1439	7	43	50
Polymixiiformes	Polymixiidae	Polymixia nobilis	1					5	5		11	11
Zeiformes	Grammicolepididae	Grammicolepis brachiusculus	1					1	1			
	Parazenidae	Stethopristes eos	1	1	3	4		2	2	4	8	12
	Zeniontidae	Cyttomimus stelgis	1								8	8
Gadiformes		Gadiformes	3							3	4	7
	Macrouridae	Coelorinchus aratrum	1	2	2	4	8	9	17	17	6	23
		Coelorinchus gladius	1							4	1	5
		Coelorinchus tokiensis	1	1	1	2					5	5
		Gadomus melanopterus	1	2		2						
		Hymenocephalus antraeus	1	5	3	8	69	16	85	2	2	4
		Macrouridae sp. 3	1				4		4			
		Macrouridae sp. 4	1	10	1	11		1	1			
		Macrouridae sp. 5	1				2	22	24			
		Malacocephalus cf. hawaiiensis	1	42	25	67	55	15	70	41	5	46
		Malacocephalus sp.	1					6	6			

		Pseudocetonurus septifer	1	ĺ			8		8			
		Ventrifossa atherodon	1	69	81	150	41	32	73	10	4	14
		Macrouridae	3	1	18	19	27	12	39	3	12	15
	Moridae	Laemonema sp.	1	1	10	1		1	1		12	10
		Physiculus grinnelli	1			•		•	•		4	4
		Physiculus nigripinnis	1							4	•	4
		Moridae	2					1	1	Ľ		'
Trachichthyiformes	Trachichthyidae	Hoplostethus crassispinus	1						•		37	37
Beryciformes	Berycidae	Beryx decadactylus	1		2	2	1	1	2		1	1
	·	Beryx splendens	1	1	-	1		11	11		48	48
		Berycidae	2	1		•		1	1		6	6
Pleuronectiformes		Pleuronectiformes	3					•	•	3	Ü	3
		Chascanopsetta crumenalis	1		1	1	1		1	4		4
		Chascanopsetta prorigera	1			-	2	1	3	5		5
		Bothidae	2				1	-	1	2		2
	Cynoglossidae	Symphurus strictus	1	4	18	22	13	9	22	14		14
Scombriformes	Gempylidae	Rexea nakamurai	1	3	6	9	1	5	6		17	17
	Trichiuridae	Benthodesmus cf. tenuis	1		-			_			1	1
Perciformes	Epigonidae	Epigonus cf. glossodontus	1	19	23	42		2	2			
	Lutjanidae	Pristipomoides filamentosus	1					7	7	1	1	2
Scorpaeniformes		Scorpaeniformes	3		2	2						
	Peristediidae	Scalicus engyceros	1				1		1	5	3	8
		Scalicus hians	1	3	5	8	15	14	29	15		15
	Scorpaenidae	Scorpaenidae sp. 6	1					1	1			
		Scorpaenidae sp. 8	1		1	1						
		Scorpaenidae	2				2		2			
Lophiiformes	Chaunacidae	Chaunax sp.	1					1	1			
	Lophiidae	Lophiodes cf. bruchius	1	2	7	9		1	1	2	2	4
		Lophiodes miacanthus	1								2	2
		Lophiidae	2								1	1
	Ogcocephalidae	Malthopsis mitrigera	1	3	23	26	3	4	7			
		Solocisquama erythrina	1	5	5	10						
		Ogcocephalidae	2				2		2			

seamount, significant differences between sides were observed only on Necker (Table S3). The NMDS ordination showed a distinguishable separation between seamounts, but it also shows a separation between sides on Necker and between sides on Pioneer. The cluster diagram showed that the S side of Necker was most similar to the W side of Pioneer and that the S side of Pioneer was most dissimilar from all other sites (Fig. 5A).

At 450 m, the model explained 78.4% of the variation with "seamount-by-side interaction" as the most important factor (28.0%), but the residuals also showed the same coefficient of variation as this factor (Table 4). The pairwise comparisons for the interaction showed that within a given side, there were differences among seamounts, except between FFS and Pioneer on the S side with a p=0.06 (Table S3). Within a given seamount, FFS and Pioneer showed significant differences between sides (Table S3). An NMDS and the cluster diagram showed that the W side of Pioneer grouped more closely with both sides of Necker than it did with the S side of Pioneer. Also, in the cluster diagram, the W side of FFS was more similar to this cluster than to the S side of FFS, and again the S side of Pioneer was the most dissimilar (Fig. 5B).

At 600 m, the model explained 78.6% of the variation with

"seamount-by-side interaction" as the most important factor (28.8%) (Table 4). The pairwise comparisons for the interaction showed that within a given side, there were differences among seamounts, except between FFS and Pioneer on the W side. Within a given seamount, there were significant differences between both sides on FFS and Pioneer (Table S3). These results are also observed in the NMDS ordination and cluster diagram, where there is an overlap of the W sides of FFS and Pioneer. In the cluster diagram, both sides of Necker were more similar to each other than to other seamounts. The cluster diagram also showed that the W sides of FFS and Pioneer overlapped and were more similar to both sides of Necker than to the S sides of either Pioneer or FFS, which again were the most divergent assemblages (Fig. 5C).

Based on the SIMPER analysis, the highest percent contribution to the dissimilarities at 300 m among seamounts and seamount sides were given by Neoscopelus macrolepidotus, Scalicus engyceros, Symphysanodon maunaloae, Chrionema squamiceps, Argyripnus sp., and Bembradium roseum (Table S4). At 450, Scorpaena pele, Symphysanodon maunaloae, C. squamiceps, Beryx splendens, and Argyripnus sp. contributed the most to the differences among seamounts and seamount sides (Table S4). At 600 m, differences among seamounts and seamount sides were given mostly by Chlorophthalmus proridens, Coelorinchus aratrum, Malthopsis mitrigera,

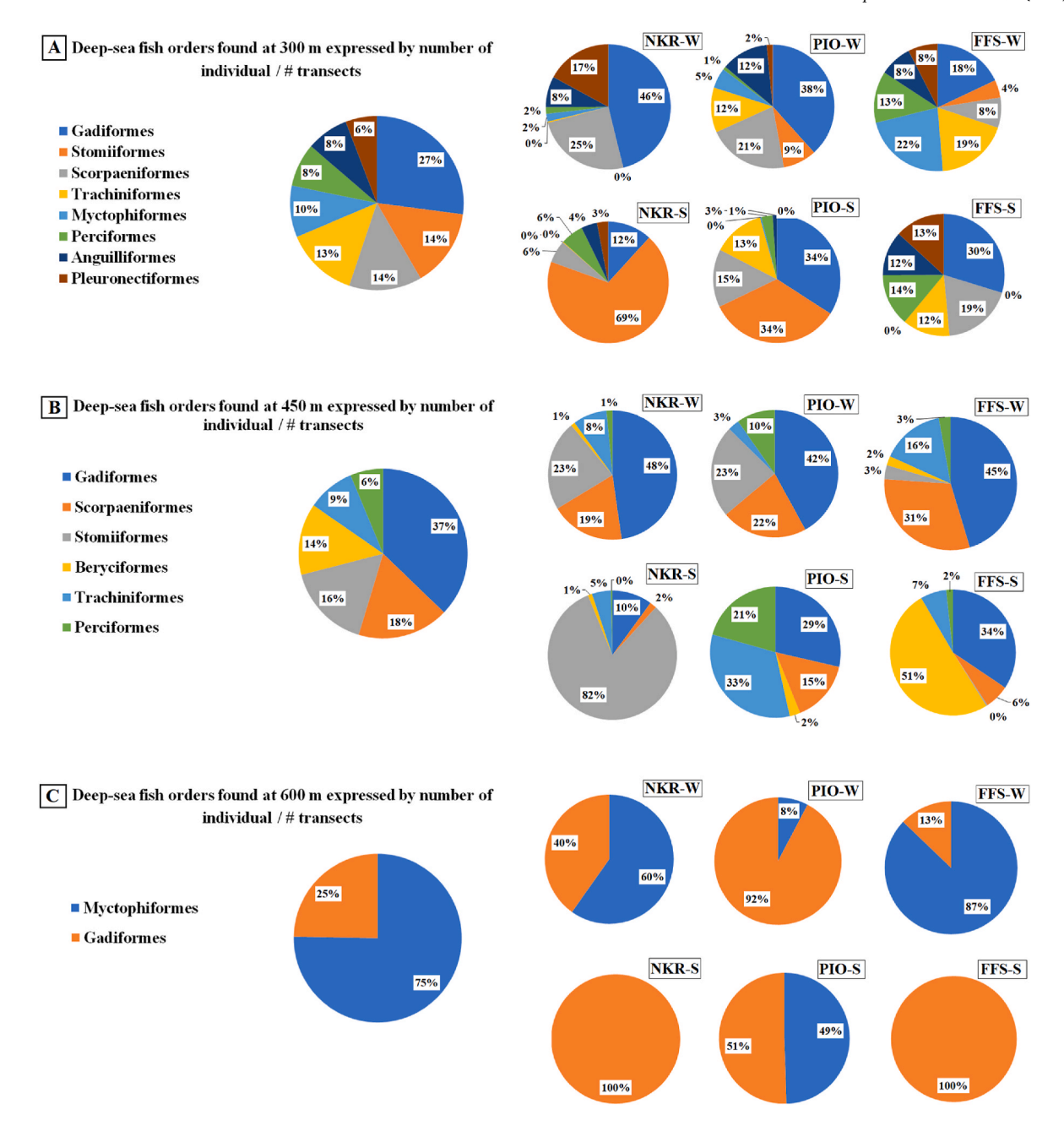


Fig. 3. The composition, based on relative abundance, of the most abundant deep-sea fish orders are shown overall and by seamount and side of the seamount at the three depths: A) 300, B) 450, and C) 600 m. Only orders with at least 5% abundance are shown. The studied seamounts are Necker Island (NKR), French Frigate Shoals (FFS), and Pioneer Bank (PIO), and the sides are represented as west (W) and south (S).

and Hymenocephalus antraeus (Table S4). Average similarities in assemblage structure observed on the S side of Necker and the W side of Pioneer at 300 m share the high contribution of the conger eel Gnathophis cf. heterognathos and the scorpionfish Bembradium roseum (Table S5). At 450 m, the most important species contributing to average similarities in both sides of Necker were the marine hatchetfish Argyripnus sp. and the duckbill Chrionema chryseres. These two species were also observed with high contributions on the W sides of FFS, while on the W side of Pioneer only Argyripnus showed a high contribution (Table S5). At 600 m, fish assemblages on the W sides of FFS and Pioneer were characterized by the high contribution of the greeneye Chlorophthalmus proridens, the grenadier Malacocephalus cf. hawaiiensis, the armored searobin Scalicus hians, and the grenadier Coelorinchus aratrum. From these species, M. cf. hawaiiensis was also found on both sides of Necker with high contributions (Table S5).

3.5. Habitat effects

After testing for high correlations ($r \ge + 0.90$ or r < -0.90) and multicollinearity (VIF <5) by depth, the remaining variables tested after the removal of colinear parameters were the following: at 300 m, time of day (sin and cosine), latitude, oxygen, salinity, direction of substrate, substrate size, % slope, POC, chl a M, and current vector u; at 450 m, time of day (sin and cosine), latitude, direction of substrate, % rugosity, substrate size, % slope, POC, chl a N, and current vector u, and at 600 m, time of day (sin and cosine), latitude, oxygen, direction of substrate, % rugosity, substrate size, % slope, POC, and chl a N.

DistLM sequential test results at 300 m showed that all variables together explain 84% of the variation in the assemblage, with time of day (sine) explaining the highest proportion of variation (25%, Table 5). After accounting for time of day, current vector u was the next most

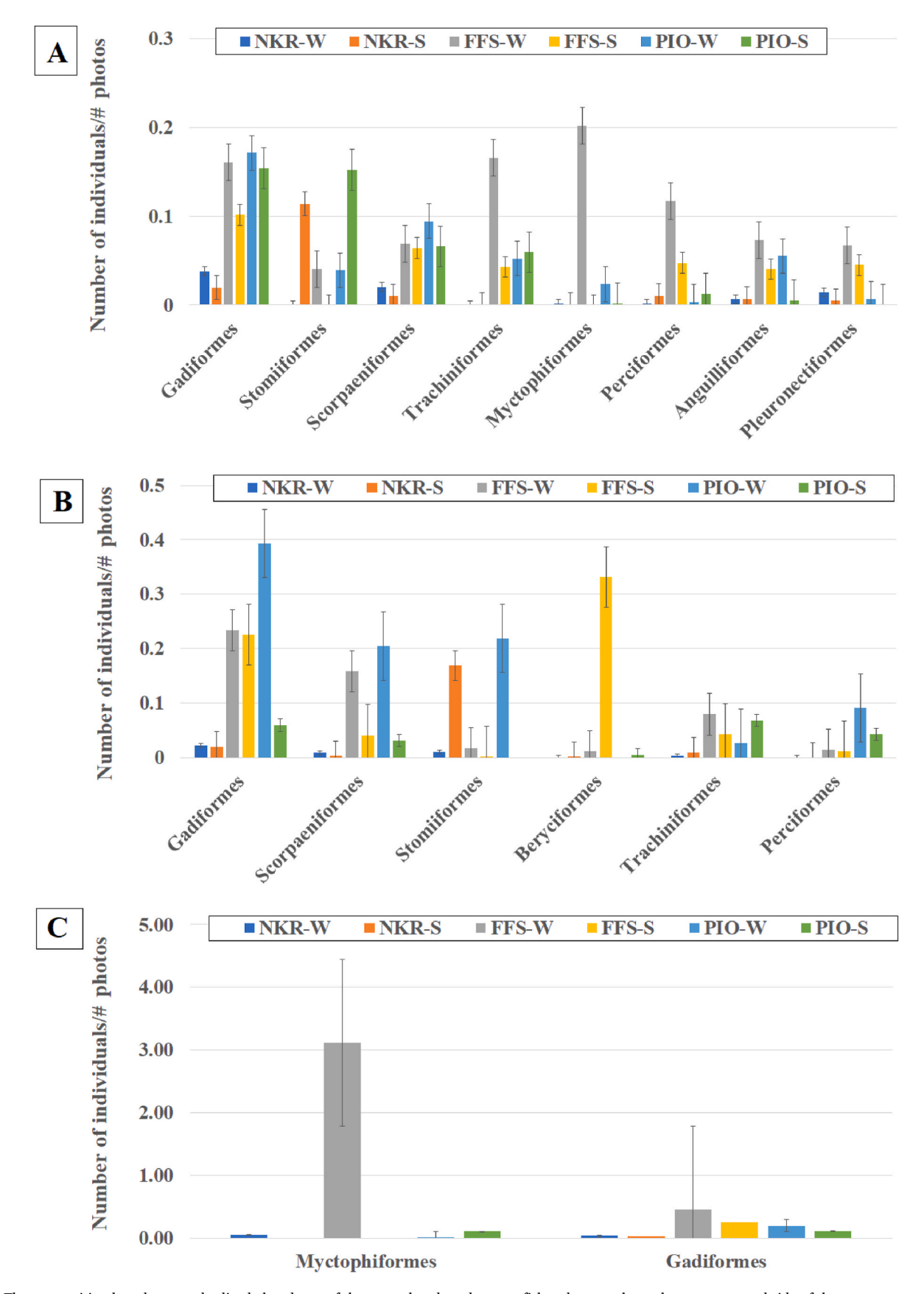


Fig. 4. The composition based on standardized abundance of the most abundant deep-sea fish orders are shown by seamount and side of the seamount at the three depths: A) 300, B) 450, and C) 600 m. Standardized abundance is expressed as the total number of individuals divided by the number of photos at each depth. Only orders with at least 5% abundance are shown. The studied seamounts are Necker Island (NKR), French Frigate Shoals (FFS), and Pioneer Bank (PIO), and the sides are represented as west (W) and south (S). Standard errors are shown.

Table 3

The deep-sea fish spatial variation using abundance (individuals/# photos), species richness (S), rarefaction estimates of the expected species richness in a 300-individual sample [ES (300)], Shannon diversity (H', nats), and Simpson dominance (D) metrics. A two-way crossed permutational analysis of variance (PERMANOVA) was used at three different depths to compare each metric among seamounts and sides using Euclidean distance and 10,000 permutations. p values < 0.05 are bolded.

300 m	Seamount df = 2		Side $df = 1$		Seamount x Side	df = 2
	Pseudo-F	p	Pseudo-F	p	Pseudo-F	p
Abundance (ind./# photos)	70.205	0.0001	10.821	0.009	17.208	<0.001
Species richness (S)	3.0522	0.083	2.4233	0.148	6.8064	0.011
Estimated species richness (Es (300))	2.7605	0.102	0.8527	0.367	3.9009	0.052
Shannon diversity (H')	1.4665	0.284	0.1907	0.725	0.5034	0.651
Simpson dominance (D)	1.0023	0.430	1.3242	0.293	0.6207	0.604
450 m	Seamount df =	2	$\overline{\text{Side df}} = 1$		Seamount x Sid	e df = 2
	Pseudo-F	p	Pseudo-F	p	Pseudo-F	p
Abundance (ind./# photos)	9.9523	0.007	0.2758	0.645	0.1915	0.866
Species richness (S)	1.5168	0.258	1.9955	0.191	1.8529	0.203
Estimated species richness (Es (300))	1.3105	0.313	2.4385	0.154	1.6173	0.245
Shannon diversity (H')	1.6305	0.243	8.8785	0.013	1.8178	0.204
Simpson dominance (D)	2.8942	0.104	9.3345	0.012	2.9676	0.101
600 m	Seamount df =	2	$\overline{\text{Side df}} = 1$	<u> </u>	Seamount x Sid	e df = 2
	Pseudo-F	p	Pseudo-F	p	Pseudo-F	p
Abundance (ind./# photos)	8.186	0.014	7.9615	0.010	8.6895	<0.001
Species richness (S)	4.3831	0.043	0.1888	0.664	1.8506	0.208
Estimated species richness (Es (300))	1.2431	0.319	0.9735	0.342	7.0409	0.012
Shannon diversity (H')	7.6368	0.010	0.3568	0.557	7.4182	0.009
Simpson dominance (D)	5.6384	0.020	0.0955	0.762	9.2093	0.005

important variable, followed by oxygen, salinity, latitude, and cosine of time. These six variables were all individually significant (p \leq 0.05) and together explain 77% of the total variation. Other variables such as substrate size, direction of substrate, and % slope added each less than 5% to the model and were not significant (p > 0.05).

At 450 m, chl a N explained the highest proportion of variation (20%, Table 5), followed by POC, current vector u, time (sine), and direction of substrate; each of which was individually significant ($p \le 0.05$), with a cumulative proportion of 66%. Other variables such as cosine of time, percent rugosity, latitude, substrate size, and percent slope were not significant but added 19% to the cumulative proportion (Table 5).

At 600 m, all variables together explained 80% of the variation in the assemblage structure (Table 5). Rugosity explained the highest proportion of variation (22%, Table 5), followed by chl a N, latitude, time of day (sine), and POC, which were all significant (p \leq 0.05) and had a cumulative proportion of 70%. The remaining variables of the cosine of time and percent slope each explained less than 5% of the variation and were not significant.

4. Discussion

Being part of one of the world's largest mountain chains (Clague and Dalrymple, 1989) and as one of the largest marine reserves, the Papahānaumokuākea Marine National Monument (PMNM) is an excellent location to gain a better understanding of seamount ecology. The PMNM has great variability in oceanographic and physiographic characteristics (Polovina et al., 1995; Firing and Brainard, 2006; Mundy, 2005) and supports a great abundance and diversity of species. This study expands on previous work examining vertical and horizontal variability of fish assemblages on individual seamounts within the PMNM (Struhsaker, 1973; Chave and Mundy, 1994; Mejía-Mercado et al., 2019; Mejía-Mercado and Baco, 2022) to look at horizontal variability within and among three seamounts.

4.1. Vehicle biases

Each type of tool used for observing mobile deep-sea species is expected to have inherent biases that can influence estimates of abundance and diversity in seamount communities (Clark et al., 2010b). Results

obtained with trawls may be biased to find species living in soft substrates. Seamounts are characterized by sandy and rocky substrates, the latter forming caves (Karig et al., 1970; Lonsdale et al., 1972) that are difficult to sample and generate a lot of loss in trawl nets (Zimmermann, 2003; personal observations). Also, trawl catchability can be affected by the escapement of some species (Somerton et al., 1999). Likewise, the use of photos and videos collected with AUVs, submersibles, and ROVs may also create biases depending on the light intensity and reflection, noise, and closeness to the organisms that can lead to both overestimates and underestimates of abundance and diversity (Tolimieri et al., 2008; Durden et al., 2016; Mejía-Mercado et al., 2019). However, human-occupied vehicles (HOVs), remotely operated vehicles (ROVs), and AUVs allow us to obtain data in very complex terrain.

Of these, AUVs, which are not tethered to the vessel (Griffiths, 2003), have been demonstrated to be good tools to study deep-sea fish communities (e.g., Tolimieri et al., 2008; Milligan et al., 2016). Unlike other underwater vehicles (see Hixon et al., 1991; Stein et al., 1992), AUVs

Table 4
A Multivariate PERMANOVA analysis of fish assemblages found at 300, 450, and 600 m on Necker Island, French Frigate Shoals, and Pioneer Bank based on a two-factor crossed model. The analysis was based on the fourth root transformed abundance data (individuals/# photos), Bray-Curtis similarity matrices, and 10,000 residual permutations. p values < 0.05 are bolded. The component of variation (C.V.) was used to determine the most important factor.

Depth	df	Pseudo-F	p (perm)	Sqrt (C.V.)	C.V. %
300 m					
Seamount	2	8.303	< 0.001	36.658	30.8
Side	1	2.7883	0.009	14.855	12.5
Seamount x Side	2	4.3865	< 0.001	35.303	29.7
Residuals	11			32.019	26.9
450 m					
Seamount	2	6.1484	< 0.001	29.321	26.9
Side	1	4.1028	< 0.001	18.64	17.1
Seamount x Side	2	3.7832	< 0.001	30.487	28.0
Residuals	11			30.501	28.0
600 m					
Seamount	2	5.9232	< 0.001	27.426	25.4
Side	1	4.9855	0.002	20.208	18.7
Seamount x Side	2	4.144	< 0.001	30.995	28.8
Residuals	11			29.176	27.1

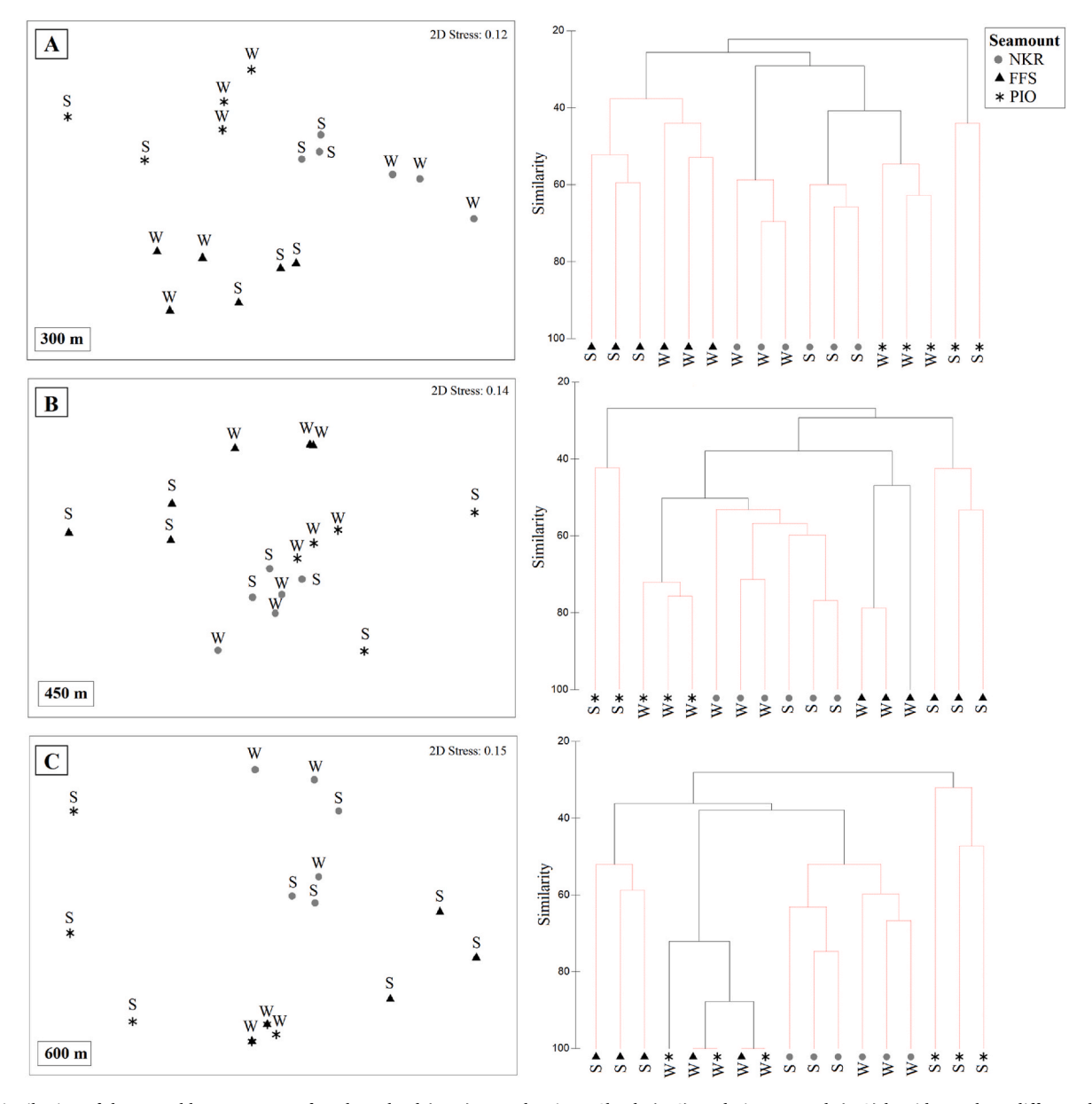


Fig. 5. Distribution of the assemblage structure of Necker Island (NKR), French Frigate Shoals (FFS), and Pioneer Bank (PIO) by sides at three different depths: A) 300 m, B) 450 m, and C) 600 m. The non-metric multidimensional scaling ordinations (NMDS) and the dendrogram of transects produced by hierarchical clustering and group average were based on Bray Curtis similarities calculated on the fourth root transformed abundance data. W and S indicate seamount sides. Each point represents a single transect. Note in panel C, the W sides of FFS and Pioneer are completely overlapping in the NMDS. Black lines in dendrograms denote significantly different clusters (SIMPROF, p < 0.05).

can survey large areas and their almost constant altitude from the bottom reduces the disruption to the benthic or demersal fish community. Also, the high-quality digital color photographs of the sea floor obtained with AUVs (Wynn et al., 2014) allow for good identification of species (Mejía-Mercado et al., 2019). However, assessing and minimizing biases in sampling methods is still critical to understanding the quality of the observations. In this study, photos that were too dark, out of focus, too high, or too close to the bottom were discarded prior to taxonomic identification to control for limitations of the methodology. In addition, the use of confidence scores helped to reduce the error of taxonomically identified organisms in which certain taxonomic characteristics such as body shape, the position of the mouth, or coloration patterns may be limited due to the mainly dorsal view of the organisms. After these quality assurance steps, 91% of the total observed fishes (7,897) were identified to a genus or species level, indicating great success in taxonomic identification from the AUV images. Additionally, the difference in the nonparametric estimators of expected species richness at the three depths was only between 7 and 8%, suggesting a representative portion of the diversity was captured with this method.

4.2. Horizontal patterns of deep-sea fish abundance and diversity

Overall, the most abundant orders of fishes at 300, 450, and 600 m on all three seamounts decreased in number with depth. Gadiformes showed the overall highest relative abundance and standardized abundance at most sites at depths of 300 and 450 m, while Myctophiformes showed the highest relative and standardized abundance at 600 m. At 300 m, Gadiformes was the dominant order based on relative abundance on Pioneer, on the W side of Necker, and the S side of FFS. Based on standardized abundance Gadiformes dominated on Pioneer and the W side of FFS. At 450 m Gadiformes dominated on the W side of all three seamounts. But Stomiiformes dominated on the S side of Necker and

Table 5 Distance-based Linear Model (DistLM) sequential test results of the spatial, temporal, and environmental variables used to evaluate correlation with the deep-sea fish assemblage structure patterns at 300, 450, and 600 m depth. A forward selection procedure and Akaike Information Criterion (AIC) were used. Bolded values indicate p values ≤ 0.05 .

300 m							
Sequential tests							
Variable	AIC	SS(trace)	Pseudo-F	p	Prop.	Cumul.	res.df
+Sin_Time	131.15	9956.7	4.9593	0.0001	0.24847	0.24847	15
+u	128.54	7158.9	4.3659	0.0001	0.17865	0.42712	14
+Oxygen	126.94	4375.7	3.0615	0.0010	0.10920	0.53632	13
+Salinity	124.74	4073.1	3.3691	0.0005	0.10165	0.63797	12
+Latitude	122.95	2897.8	2.7456	0.0039	0.07231	0.71028	11
+Cos_Time	121.38	2197.6	2.335	0.0077	0.05484	0.76512	10
+Substrate size	121.29	1090.0	1.1788	0.3205	0.02720	0.79232	9
+Direction substrate	121.09	1007.9	1.1024	0.3773	0.02515	0.81748	8
+%Slope	120.47	1044.3	1.166	0.3421	0.02606	0.84354	7
450 m							
Sequential tests							
Variable	AIC	SS(trace)	Pseudo-F	p	Prop.	Cumul.	res.df
+chla Nesdis	128.43	6385.5	3.7337	0.0005	0.19930	0.19930	15
+POC	127.26	4366.2	2.8715	0.0056	0.13628	0.33558	14
+u	125.73	3988.0	2.9969	0.0009	0.12447	0.46005	13
+Sin_Time	124.23	3218.4	2.7428	0.0046	0.10045	0.56051	12
+Direction substrate	122.04	3074.6	3.0728	0.0034	0.09596	0.65647	11
+Cos_Time	120.87	1873.8	2.0518	0.0636	0.05849	0.71496	10
+%Rugosity	119.80	1510	1.7829	0.0926	0.04713	0.76209	9
+Latitude	119.07	1130.7	1.3933	0.2234	0.03529	0.79738	8
+Substrate size	119.00	742.54	0.9041	0.5213	0.02318	0.82055	7
+%Slope	117.63	1034.8	1.3169	0.2780	0.03230	0.85285	6
600 m		· <u> </u>		' <u></u>			
Sequential tests							
Variable	AIC	SS(trace)	Pseudo-F	p	Prop.	Cumul.	res.df
+%Rugosity	127.37	6844.1	4.2589	0.0007	0.22114	0.22114	15
+chla Nesdis	125.07	5387.4	4.0296	0.0027	0.17407	0.39521	14
+Latitude	122.58	4341.1	3.9255	0.0015	0.14027	0.53548	13
+Sin_Time	120.43	3112.9	3.3164	0.0017	0.10058	0.63606	12
+POC	118.92	2105.9	2.5295	0.0254	0.06804	0.70410	11
+Cos_Time	117.82	1524.1	1.9965	0.0929	0.04925	0.75335	10
+%Slope	116.57	1330.1	1.8991	0.1060	0.04298	0.79633	9

Beryciformes on the S side of FFS. At 600 m, Myctophiformes showed the highest abundance on the W sides of Necker and FFS. A higher abundance of Gadiformes among other orders would be expected at the three sampled depths as Gadiformes is known to be a dominant order in the general deep sea (Priede, 2017). However, the highest abundance of Myctophiformes at 600 m was greater than the abundance of Gadiformes. Myctophiformes, with only one species N. macrolepidotus, accounted for more than half of the overall abundance on one side of FFS that was sampled mostly during the night. Most species that belong to Myctophiformes are considered mesopelagic, migrating to the surface to feed during the night and hiding from predators at deeper depths during the day. However, N. macrolepidotus is known to be a demersal myctophid that spends most of its life close to the bottom over continental and island slopes that offer food resources (Nafpaktitis, 1977; Bekker and Shcherbachev, 1990) without migrating vertically (Nafpaktitis, 1977). Thus, the observation of this species in such close association with the seafloor in this study supports its demersal lifestyle strategy.

The dominant orders in this study based on standardized abundance also varied from one seamount to another and from one side to another at each sample depth. At 300 m, three of the eight orders (Gadiformes, Stomiiformes, and Scorpaeniformes) were observed with the highest abundance on Pioneer on either side, while the other five orders showed the highest abundance on French Frigate Shoals (FFS) on the west side. Similarly, at 600 m, two orders showed the highest abundance on FFS, on the W side. Unlike these two depths, at 450 m, three of the six orders (Gadiformes, Scorpaeniformes, and Trachiniformes) showed similar abundances in FFS and Pioneer, but differently on either side of each seamount. One might expect that the proximity of Necker and FFS (ca. 155 km), regardless of depth, would cause these two seamounts to have

a more similar distribution of orders, rather than FFS and Pioneer which are approximately 900 km apart, as we observed in this study.

Significant differences in standardized fish abundance by seamount, side, and the interaction were observed at 300 and 600 m, while at 450 m abundance was different only by seamount. This variability in fish abundance corresponds with the variability in abundance by side within a single seamount observed in previous studies in the Monument at similar depths (Mejía-Mercado et al., 2019; Mejía-Mercado and Baco, 2022) and from one seamount to another in a study conducted in New Zealand at deeper depths (Tracey et al., 2012). In the current study, abundance was higher on FFS than on the other two seamounts at all three depths with higher abundance on the W side at 300 and 600 m. Phytoplankton biomass has been found to increase over seamounts in the tropical and subtropical Pacific with summit depths deeper than 30 m, leading to higher catches, including the seamounts of this study (Leitner et al., 2020). Horizontal variability in fish abundance has also been associated with site-specific topographic and oceanic conditions (Mejía-Mercado et al., 2019) that determine the amount of food supply in the area and at a given depth (Rogers, 1994; Genin, 2004). Unlike the other two seamounts, FFS is the remaining part of an atoll with a well-developed barrier reef and lagoon (Kenyon et al., 2006). It has been shown that islands and atolls with well-developed coral reefs can experience enhanced primary productivity due to the island mass effect (Gove et al., 2016). FFS has the biggest reef habitat in the Hawaiian Archipelago due to the existence of atoll and basalt structures (Grigg and Dollar, 1980; Maragos and Gulko, 2002) that are located on the east side (Miller et al., 2003), with an extensive lagoon on the west side. Therefore, the high abundance of organisms that was observed on the W side of FFS at 300 m depth may be benefiting from the high productivity generated on the reef habitats, which is flushed across the reef from east to west (Gove et al., 2016).

Species richness was only significantly different by the interaction of seamount and side at 300 m, but in general, there were more differences in the diversity metrics by the interaction of factors at 600 m than at the other two depths. The occurrence of fish species in a specific depth range has been observed to be determined by the physiological adaptations of the species to physical and chemical conditions of the environment (e.g., Chave and Mundy, 1994; Yeh and Drazen, 2009), which in Hawaii change considerably in the water column above 1000 m depth (Chiswell, 2002). However, when considering the horizontal scale, other studies have shown that substrate characteristics in conjunction with the flow regime can be correlated with species composition in an area due to habitat preferences (Borland et al., 2021; Mejía-Mercado and Baco, 2022). The differences that were observed at 300 m between Necker and FFS on their S sides seem to be related mostly to differences in substrate parameters. While both sides had similar mean values in the physico-chemical conditions and surface current vectors, the substrate of the S side of Necker had a sandier substrate with low rugosity compared to the S side of FFS. Flatfishes (e.g., Chascanopsetta crumenalis, Taeniopsetta radula, and Symphurus strictus), batfishes (e.g., Halieutaea retifera and Malthopsis mitrigera), and sea robins (Scalicus engyceros) that increased the number of species on this side may prefer the higher mean proportions of sandy substrate. At 600 m depth, differences in diversity were observed mainly between the S sides of FFS and Pioneer, with the highest diversity and the lowest dominance on the S side of FFS. While the S side of Pioneer is a pinnacle that has a very narrow shelf, the S of FFS presents an extended shelf. These differences in geomorphology may interact with currents in the area to determine the most favorable habitat for some species (Borland et al., 2021), which may be the case for the S side of FFS.

4.3. Patterns of deep-sea fish assemblage structure

At all depths, the fish assemblage structure showed significant variation among seamounts and sides that was mostly explained by the interaction term. These results support previous seamount studies, where the composition and abundance of organisms varied from one seamount to another driven by differences in the environmental conditions of each seamount (Richer de Forges et al., 2000; Tracey et al., 2004, 2012; McClain, 2007; Morato and Clark, 2007; Rowden et al., 2010; Clark et al., 2010a, 2010b, 2012; Schlacher et al., 2014), but this study is the first to quantitatively test for differences while controlling for depth.

The similarities among sides of different seamounts differed among depths and did not match expectations based on distances among seamounts. At 300 and 450 m, Necker was most similar to the W side of Pioneer, while FFS, which is the closer seamount to Necker, was less similar to either seamount. At 600 m, the W side of FFS formed a mixed cluster with the W side of Pioneer, before the two clustered with both sides of Necker. At all depths, the S side of Pioneer was the most divergent from all other seamounts and sides, and at 450 and 600 m the S side of FFS was also highly divergent from all others. The S side of Pioneer may have been the most divergent because the transects were conducted on a small pinnacle of the bank that represents different geomorphology. Nevertheless, the available environmental data for this side of the seamount did not show strongly different patterns from any of the other seamount sides.

Besides the smaller geographic distance, surface currents also create an expectation of greater similarity between FFS and Necker. FFS and Necker are part of the middle portion of the Archipelago that is connected by the STCC which flows eastwards (Kobashi and Kawamura, 2002), while Pioneer is part of the northwestern portion of the NWHI that is influenced by a current flowing northeast between Pearl and Hermes and Pioneer Bank (Firing and Brainard, 2006). Thus, similarities between Necker and the W side of Pioneer at 300 and 450 m are

unexpected. Necker and the W side of Pioneer assemblages were characterized by *Gnathophis* cf. *heterognathos* and *Bembradium roseum* at 300 m and *Argyripnus* sp. at 450 m.

Based on the NMDS plot in Fig. 5c, at 600 m there were strong similarities in the assemblage structure between the W sides of FFS and Pioneer. The NHRC, a current that reaches to 200 m depth and flows westward, has been described as an important mechanism for the transportation of phytoplankton and zooplankton (Hirota et al., 1980), as well as larvae (Polovina et al., 1995; Kobayashi and Polovina, 2006) from the MHI toward the NWHI (Firing and Brainard, 2006; Desch et al., 2009). This surface current is likely to act as a mechanism of distribution for taxa with epipelagic eggs or larvae. Nevertheless, deeper currents passing FFS and flowing westwards, or close to Pioneer and flowing eastwards, could also be involved in these similarities. Therefore, it is important to conduct more studies focused on currents at depths below 300 m to better understand the mechanisms behind the distribution of species along the seamounts in the Monument.

4.4. Variables correlated to the structure of the assemblages

Although the PCA analyses of the environment at each depth showed the highest variability in the current vector \mathbf{u} , chl a, temperature, percent sand, and oxygen, these variables were only some of the variables that were correlated to the community structure variation as tested by DistLM.

Although time of day did not show up as an important variable in the individual analyses of either Pioneer Bank or Necker Island (Mejía-Mercado et al., 2019; Mejía-Mercado and Baco, 2022), in the current analyses it came out significant at the three depths and with the highest proportion of explanation at 300 m. Time of day has the potential to confound the overall analyses as a sampling artifact, particularly at 300 m. Time of day is expected to control vertical patterns of distribution of fishes when the assemblage includes species that have a vertical migration in the water column (see Reid et al., 1991).

However, in this case, the effect of time of day is not so clear cut as being simply a function of diel vertical migrators (DVM). As discussed in Section 4.2, the main species of Myctocphiiformes present on these seamounts, N. macrolepidotus, shows no evidence of vertical migration (Nafpaktitis, 1977). Another group expected to include DVM are the Stomiiformes. At 300 m, the stomiid, Argyripnus spp., was one of the species with a major contribution to the dissimilarities among seamounts and seamounts sides. Argyripnus spp., has been fished with bottom trawls at mesopelagic depths but near the sea floor (Harold and Lancaster, 2003). In this study, Argyripnus spp. showed high relative abundances on the S side of Pioneer and Necker which were sampled during the night, but at the same time, it was absent from the W side of Necker which was also sampled during the night. At 600 m, of the species that had a high % contribution in dissimilarities, most of them are benthic species, while the other two, which are macrourids, are known as demersal species but lack information on vertical migration. Therefore, DVM do not appear to be a major component of the assemblages of fishes observed. To support this assertion, a reanalysis of the data with the Myctophiformes and Stomiiformes removed still yielded time of day as a significant variable in the DISTLM (results not shown). Similarly, additional analyses with these two orders and all other taxa that might be considered DVM removed also continued to yield time of day as a key component of the DISTLM results (results not shown).

While making the current analyses more complicated, these results also provide interesting insights into the effects of time of day on benthic and demersal deep-sea species. Besides diel vertical migration, light intensity is also associated with the rhythmic behavior of benthic species (Aguzzi et al., 2015) and it is quite common in shallow water, e.g. on a shallow tropical reef, to have a different suite of species present at night compared to during the day (e.g. Campanella et al., 2019). Therefore, having time of day be a part of the significant factors in the DISTLM, indicates that at 300 and 450 m and even to depths 600 m, there is an

influence of light on the active community of fishes at a given time of day.

Another potential confounding factor in this study is spatial autocorrelation, in which sites that are closer to each other are more similar than sites further apart. Latitude is a proxy for distance and came out as a significant variable at 300 (7% of variation) and 600 m (14%). Latitude, which was highly correlated with longitude, can also influence the community structure due to differences in environmental factors, such as average temperature that can also be related to dissolved oxygen (Rohde, 1992). A previous study on seamounts in New Zealand reported base depth, which was highly correlated with latitude, being one of the most important environmental variables influencing the structure of the fish assemblages on seamounts as little as 8 km apart (Tracey et al., 2012). In this study, we have seamounts separated at least 155 km, which may explain the importance of this variable influencing the structure of assemblages. However, the similarities in assemblage structure observed between the S side of Necker and the W side of Pioneer do not support the idea of spatial autocorrelation. Even more, at 600 m, the NMDS ordination and cluster diagram showed an overlap of the W sides of FFS and Pioneer. Therefore, these similarities between distant sides of different seamounts are more likely to be a result of different environmental variables' influence.

After accounting for time of day and latitude, another variable that came up as significant was surface current vector u (east-west flow) at 300 and 450 m. Surface currents have been observed to influence the differences in assemblage structure on seamounts (Genin, 2004) On one hand, surface currents may influence the larval dispersal of some benthic fish species (Koslow et al., 1994; Francis et al., 2002). On the other hand, currents can interact with the slope to determine the amount of organic material moving vertically or horizontally on seamounts (Genin and Boehlert, 1985). At 300 m, differences in the assemblage structure were observed between Pioneer and the other two seamounts, so the slower east-west surface currents that were observed on Pioneer may be influencing these differences. At 450 m, there was not a clear pattern in the current vector u that may be associated with the differences in the assemblage. However, more studies that include deep currents would be important to understand the effect of currents acting at different depths on deep-sea fish assemblages.

Chl a N and POC were the variables explaining the highest proportion of variation at 450 m and were also among the significant variables at 600 m. Chl a and POC can show a significant increase on seamounts compared to the surrounding oceanic conditions (Leitner et al., 2020) and are highly available in the upper water column, decreasing with depth (Suess, 1980). Both variables are highly influenced by physical processes such as advection and water column stratification that can affect their concentrations both vertically and horizontally (White et al., 2007). Likewise, horizontal or vertical migration of fishes can contribute to the dissemination of these two variables (Holmlund and Hammer, 1999), which also can be influenced by the structure of the fish community (see Milligan et al., 2020). These events eventually will influence the abundance and composition of benthic species inhabiting a certain area. In the present study, FFS showed the highest surface values of chl a (extracted from Nesdis) and POC, and at the same time a higher abundance and high diversity compared to the other two seamounts. A caveat of this work is that a single time point is represented for fishes, while chl a and POC are averaged across eight years. It is important to consider temporal variations in the concentrations of chl a and POC and their relation to community structure e.g. Milligan et al. (2020) reported the highest abundance of demersal fishes four months after a peak in primary production. Therefore, a study of the same sites at multiple times in a year might reveal different patterns.

Percent rugosity explained the largest portion of variation at 600 m. Percent rugosity has been directly associated with assemblage structure, likely due to fish habitat preferences (Mejía-Mercado et al., 2019; Mejía-Mercado and Baco, 2022), but also with variations in the abundance and composition of fishes (Kelley et al., 2006; Oyafuso et al.,

2017) and invertebrates (Long and Baco, 2014; Morgan et al., 2019). The low rugosity that characterized the W sides of FFS and Pioneer appears to be influencing their similarity in assemblage structure, but it also appears to influence their differences with other sides on the same seamounts and different seamounts.

Additional environmental factors for at least one depth included oxygen and salinity at 300 m and mean direction of substrate at 450 m. Oxygen and salinity that are correlated with temperature are potential driving factors as they have been shown to influence the physiology, metabolism, and life history cycle of organisms (Thistle, 2003; Clark et al., 2010b). Oxygen and salinity, which vary with depth, have been associated with vertical changes in the composition of fish assemblages (Wishner et al., 1990; Yeh and Drazen, 2009; Mejía-Mercado et al., 2019) and invertebrates (Morgan et al., 2019). However, oxygen and salinity concentrations, like temperature, can also vary horizontally at a given depth due to the influence of currents and circulation (Randall and Farrell, 1997). In the present study, noticeable variability in oxygen concentrations was observed at 300 m on both sides of Pioneer, showing the highest and lowest average values (S = 8.0 mg/l (SD = 0.09) and W =6.7 mg/l (SD =0.05)) among the other sites, and likely influencing assemblage structure within Pioneer, or between either side of Pioneer and any sides of the other seamounts.

Mean direction of substrate that was significant at 450 m, was obtained from aspect, or the face of the slope, and was also a significant factor correlated to community structure in the focused study of Pioneer Bank (Mejía-Mercado and Baco, 2022). The direction of the slope will affect interactions with deep-water currents, potentially having effects on the substrate and food supply that may contribute to differences in the fish assemblage structure within seamounts. There is a lack of information related to mean direction of the substrate and variation in fish assemblages, which may be a fruitful direction for further research.

5. Conclusions

This is the first study to quantitatively analyze horizontal patterns of distribution of seamount fish assemblages while controlling for depth, and in the PMNM, the first study to consider seamounts separated by a maximum distance of 900 km. From three seamounts we show horizontal variability in fish abundance, diversity, and assemblage structure between sides within a single seamount as well as between sides of different seamounts at 300, 450, and 600 m depth. Differences in diversity metrics among seamounts were higher at 600 m than at the other two depths. Assemblage structure at all three depths was correlated with time of day, but current vector u, latitude, chl a, and POC were also highly correlated. In some cases, one side of a seamount was more similar to another seamount than to the other side on the same seamount. Additionally, similarities were higher among distant seamounts than closer seamounts. These results suggest complex patterns of connectivity within the seamount chain, with potentially higher connectivity between similar sides of different seamounts than among sides of the same seamount, independent of geographic distance. These patterns seem to be associated with similar substrate parameters and species' habitat preferences, but deep currents could influence similar patterns along the seamounts. These findings can be used to improve management decision-making in the Monument and other areas as it constitutes a basis for understanding horizontal distribution patterns in deep-sea fishes at seamounts that are relatively unaltered by human activity.

Declaration of competing interest

The authors declare that they have no known competing financial interests or personal relationships that could have appeared to influence the work reported in this paper.

Data availability

Data are all in the supplemental file

Acknowledgments

This work was supported by NSF grant #s OCE-1334652 to ARB and OCE-1334675 to E. Brendan Roark. Work in the Papahānaumokuākea Marine National Monument was conducted under permit #PMNM-2014-028. BMM was supported by a fellowship from Colciencias-Fulbright. We thank Bruce Mundy for helping in the identification of the fish species as well as helping with the revision of the manuscript. We thank the crews of the AUV Sentry, the RV Sikuliaq, and the RV Kilo Moana. Nicole Morgan partitioned the AUV dives into transects and compiled the environmental data by transect. Surface Chlorophyll *a*, particulate organic carbon, and current vectors by transect were obtained from previous studies by Mauricio Silva. Florida State University undergraduate students Allison Metcalf and Kelly Klein helped with substrate description.

Appendix A. Supplementary data

Supplementary data to this article can be found online at https://doi.org/10.1016/j.dsr.2023.104003.

References

- Aguzzi, J., Sbragaglia, V., Tecchio, S., Navarro, J., Company, J.B., 2015. Rhythmic behaviour of marine benthopelagic species and the synchronous dynamics of benthic communities. Deep Sea Res. Pt. I 95, 1–11.
- Akaike, H., 1973. Information theory as an extension of the maximum likelihood principle. In: Petrov, B.N., Csaki, F. (Eds.), Second International Symposium on Information Theory. Akademiai Kiado, Budapest, pp. 267–281.
- Anderson, M.J., Gorely, R.N., Clarke, K.R., 2008. PERMANOVA+Primer: Guide to Software and Statistical Methods. Primer-E, Plymouth, p. 214.
- Baco, A.R., 2007. Exploration for deep-sea corals on North Pacific seamounts and islands. Oceanography 20 (4), 108–111.
- Baco, A.R., Morgan, N.B., Roark, E.B., 2020. Observations of vulnerable marine ecosystems and significant adverse impacts on high seas seamounts of the Northwestern Hawaiian Islands and Emperor Seamount Chain. Mar. Policy 115, 103234
- Baco, A.R., Morgan, N., Roark, E.B., Silva, M., Shamberger, K.E., Miller, K., 2017.
 Defying dissolution: discovery of deep-sea scleractinian coral reefs in the North Pacific. Sci. Rep. 7 (1), 5436.
- Baco, A.R., Roark, E.B., Morgan, N.B., 2019. Amid fields of rubble, scars, and lost gear, signs of recovery observed on seamounts on 30-40 year time scales. Sci. Adv. 5, eaaw4513.
- Bekker, V.E., Shcherbachev, Yu.N., 1990. Bathypelagic species of the families Neoscopelidae and Myctophidae from the Indian Ocean, with a description of a new species of *Diaphus*. J. Ichthyol. 30, 122–134.
- Beyer, H.L., 2012. Geospatial modelling environment (Version 0.7.2.0) (software). URL: http://www.spatialecology.com/gme.
- Blair, T.C., McPherson, J.G., 1999. Grain-size and textural classification of coarse sedimentary particles. J. Sediment. Res. 69 (1), 6–19.
- Borland, H.P., Gilby, B.L., Henderson, C.J., Leon, J.X., Schlacher, T.A., Connolly, R.M., Pittman, S.J., Sheaves, M., Olds, A.D., 2021. The Influence of Seafloor Terrain on Fish and Fisheries: A Global Synthesis. Fish Fish. https://doi.org/10.1111/faf.12546.
- Campanella, F., Auster, P.J., Taylor, J.C., Munoz, R.C., 2019. Dynamics of predator-prey habitat use and behavioral interactions over diel periods at sub-tropical reefs. PLoS One 14 (2), e0211886.
- Carpenter, K.E., Niem, V.H., 1998. FAO Species Identification Guide for Fishery Purposes. The Living Marine Resources of the Western Central Pacific. Cephalopods, Crustaceans, Holothurians and Sharks, vol. 2. FAO, Rome, pp. 687–1396.
- Carpenter, K.E., Niem, V.H., 1999a. FAO Species Identification Guide for Fishery Purposes. The Living Marine Resources of the Western Central Pacific. Batoid Fishes, Chimaeras and Bony Fishes Part 1 (Elopidae to Linophrynidae), vol. 3. FAO, Rome, pp. 1398–2068.
- Carpenter, K.E., Niem, V.H., 1999b. FAO Species Identification Guide for Fishery Purposes. The Living Marine Resources of the Western Central Pacific. Bony Fishes Part 2 (Mugilidae to Carangidae), vol. 3. FAO, Rome, pp. 2069–2790.
- Carpenter, K.E., Niem, V.H., 2001a. FAO Species Identification Guide for Fishery Purposes. The Living Marine Resources of the Western Central Pacific. Bony Fishes Part 3 (Menidae to Pomacentridae), vol. 3. FAO, Rome, pp. 2791–3380.
- Carpenter, K.E., Niem, V.H., 2001b. FAO Species Identification Guide for Fishery Purposes. The Living Marine Resources of the Western Central Pacific. Bony Fishes Part 4 (Labridae to Latimeriidae), Estuarine Crocodiles, Sea Turtles, Sea Snakes, and Marine Mammals, vol. 3. FAO, Rome, pp. 3381–4218.

- Chave, E.H., Mundy, B.C., 1994. Deep-sea benthic fish of the Hawaiian archipelago, cross seamount, and johnston atoll. Pac. Sci. 48 (4), 367–409.
- Chave, E.H., Malahoff, A., 1998. In Deeper Waters: Photographic Studies of Hawaiian Deep-Sea Habitats and Life-Forms. University of Hawaii Press, Honolulu, HI.
- Chatterjee, S., Hadi, A.S., Price, B., 2000. Regression Analysis by Example. John Wiley and Sons, New York, USA
- Chiswell, S.M., 2002. Energy levels, phase, and amplitude modulation of the baroclinic tide off Hawaii. J. Phys. Oceanogr. 32 (9), 2640–2651.
- Clague, D.A., Dalrymple, G.B., 1989. Tectonics, geochronology, and origin of the Hawaiian-Emperor volcanic chain. Geol. N. Am. 188–217.
- Clark, M.R., Althaus, F., Williams, A., Niklitschek, E., Menezes, G., Hareide, N.-R., Sutton, P., O'Donnell, C., 2010a. Are deep-sea fish assemblages globally homogenous? Insights from seamounts. Mar. Ecol. 31 (Suppl. 1), 39–51.
- Clark, M.R., Rowden, A.A., Schlacher, T., Williams, A., Consalvey, M., Stocks, K.I., Rogers, A.D., O'Hara, T.D., White, M., Shank, T.M., Hall-Spencer, J.M., 2010b. The ecology of seamounts: structure, function, and human impacts. Ann. Rev. Mar. Sci 2, 253–278.
- Clark, M.R., Watling, L., Rowden, A.A., Guinotte, J.M., Smith, C.R., 2011. A global seamount classification to aid the scientific design of marine protected area networks. Ocean Coast. Manag. 54 (1), 19–36.
- Clark, M.R., Schlacher, T.A., Rowden, A.A., Stocks, K.I., Consalvey, M., 2012. Science priorities for seamounts: research links to conservation and management. PLoS One 7 (1), e29232.
- Clarke, K.R., Warwick, R.M., 2001. Change in Marine Communities: an Approach to Statistical Analysis and Interpretation, second ed. Primer- E, Plymouth.
- Colwell, R.K., Coddington, J.A., 1994. Estimating terrestrial biodiversity through extrapolation. Philos. Trans. R. Soc. Lond., B. Biol. Sci. 345 (1311), 101–118.
- DeMartini, E.E., Parrish, F.A., Parrish, J.D., 1996. Interdecadal change in reef fish populations at French Frigate Shoals and Midway Atoll, Northwestern Hawaiian Islands: statistical power in retrospect. Bull. Mar. Sci. 58 (3), 804–825.
- DeMartini, E.E., 2004. Habitat and endemism of recruits to shallow reef fish populations: selection criteria for no-take MPAs in the NWHI Coral Reef Ecosystem Reserve. Bull. Mar Sci. 74 (1), 185–205.
- Desch, A.T., Wynne, T., Friedlander, A., Christensen, J., 2009. Oceanographic and physical setting. In: Friedlander, A., Keller, K., Wedding, L., Clarke, A., Monaco, M. (Eds.), A Marine Biogeographic Assessment of the Northwestern Hawaiian Islands. NOAA Technical Memorandum NOS NCCOS 84. Prepared by NCCOS's Biogeography Branch in Cooperation with the Office of National Marine Sanctuaries Papahānaumokuākea Marine National Monument. Silver Spring, MD, p. 363.
- Durden, J.M., Schoening, T., Althaus, F., Friedman, A., Garcia, R., Glover, A.G., Bett, B.J., 2016. Perspectives in visual imaging for marine biology and ecology: from acquisition to understanding. Oceanogr. Mar. Biol. 54, 1–72.
- Esri (Environmental System Research Institute, Inc.), 2016. ArcGIS Desktop: Release 10.4.1. Environmental Systems Research Institute, Redlands, CA.
- Evenhuis, N.L., Eldredge, L.G., 2004. Natural history of nihoa and necker islands. A Hawaii biological survey handbook. Bishop Mus. Bull. Cultural Environ. Stud. I 220.
- Firing, J., Brainard, R.E., 2006. Ten years of shipboard ADCP measurements along the Northwestern Hawaiian Islands. Atoll Res. Bull. 543, 347–363.
- Fisher, N.I., 1995. Statistical Analysis of Circular Data. Cambridge University Press, Cambridge, UK.
- Fofonoff, N.P., Millard Jr., R.C., 1983. Algorithms for computation of fundamental properties of seawater. Endorsed by unesco/SCOR/ICES/IAPSO joint panel on oceanographic tables and standards and SCOR working group 51. UNESCO Tech. Pap. Mar. Sci. 44.
- Francis, M.P., Hurst, R.J., McArdle, B.H., Bagley, N.W., Anderson, O.F., 2002. New Zealand demersal fish assemblages. Environ. Biol. Fish. 65, 215–234.
- Froese, R., Sampang, A., 2004. Taxonomy and biology of seamount fishes. In: Morato, T., Pauly, D. (Eds.), Seamounts: Biodiversity and Fisheries, vol. 12, pp. 25–32, 5. Fisheries Centre Research Reports. Canada.
- Genin, A., 2004. Bio-physical coupling in the formation of zooplankton and fish aggregations over abrupt topographies. J. Mar. Syst. 50 (1–2), 3–20.
- Genin, A., Boehlert, G.W., 1985. Dynamics of temperature and chlorophyll structures above a seamount: an oceanic experiment. J. Mar. Res. 43 (4), 907–924.
- Gove, J.M., McManus, M.A., Neuheimer, A.B., Polovina, J.J., Drazen, J.C., Smith, C.R., Merrifield, M.A., Friedlander, A.M., Ehses, J.S., Young, C.W., Dillon, A.K., 2016. Near-island biological hotspots in barren ocean basins. Nat. Commun. 7 (1), 1–8.
- Griffiths, G., 2003. Technologies and Applications of Autonomous Underwater Vehicles. Taylor and Francis, London, p. 360.
- Grigg, R.W., Dollar, S.J., 1980. The status of reef studies in the Hawaiian Archipelago. In: Grigg, R.W., Pfund, R.T. (Eds.), Proceedings of the Symposium on the Status of Resource Investigations in the Northwestern Hawaiian Islands. UH Sea Grant College, Honolulu, pp. 100–120.
- Haight, W.R., Kobayashi, D.R., Kawamoto, K.E., 1993. Biology and management of deepwater snappers of the Hawaiian archipelago. Mar. Fish. Rev. 55, 17–24.
- Harold, A.S., Lancaster, K., 2003. A New Species of the Hatchetfish Genus Argyripnus (Stomiiformes: Sternoptychidae) from the Indo-Pacific. Proc. Biol. Soc, vol. 116, pp. 883–891, 4.
- Hirota, J., Taguchi, S., Shuman, R.F., Jahn, A.E., 1980. Distributions of plankton stocks, productivity, and potential fishery yield in Hawaiian waters. In: Grigg, R.W., Pfund, R.T. (Eds.), Proceedings of the Symposium on Status of Resource Investigations in the Northwestern Hawaiian Islands. UH Sea Grant College, pp. 191–203.
- Hixon, M.A., Tissot, B.N., Pearcy, W.G., 1991. Fish Assemblages of Rocky Banks of the Pacific Northwest. OCS Study MMS 91-0052. US Department of the Interior, Mineral Management Service, Camarillo, California.
- Holmlund, C.M., Hammer, M., 1999. Ecosystem services generated by fish populations. Ecol. Econ. 29, 253–268.

- Karig, D.E., Peterson, M.N.A., Short, G.G., 1970. Sediment-capped guyots in the mid-pacific mountains. Deep Sea Res. Oceanogr. Abstr. 17 (2), 373–378.
- Kelley, C.H., Moffitt, R.B., Smith, J.R., 2006. Mega-to micro-scale classification and description of bottomfish essential fish habitat on four banks in the Northwestern Hawaiian Islands. Atoll Res. Bull. 543, 319–332.
- Kenyon, J.C., Vroom, P.S., Page, K.N., Dunlap, M.J., Wilkinson, C.B., Aeby, G.S., 2006. Community structure of hermatypic corals at French Frigate Shoals, Northwestern Hawaiian Islands: capacity for resistance and resilience to selective stressors. Pac. Sci. 60 (2), 153–176.
- Kobashi, F., Kawamura, H., 2002. Seasonal variation and instability nature of the North pacific subtropical countercurrent and the Hawaiian lee countercurrent. J. Geophys. Res. Oceans 107 (C11), 6–1.
- Kobayashi, D.R., Polovina, J.J., 2006. Simulated seasonal and interannual variability in larval transport and oceanography in the Northwestern Hawaiian Islands using satellite remotely sensed data and computer modeling. Atoll Res. Bull. 543, 365–390
- Koslow, J.A., Bulman, C.M., Lyle, J.M., 1994. The mid-slope demersal fish community off southeastern Australia. Deep-Sea Res. Pt. I 41 (1), 113–141.
- Leitner, A.B., Neuheimer, A.B., Drazen, J.C., 2020. Evidence for long-term seamount-induced chlorophyll enhancements. Sci. Rep. 10 (1), 1–10.
- Lonsdale, P.F., Normark, W.R., Newman, W.A., 1972. Sedimentation and erosion on Horizon Guyot. Geol. Soc. Am. Bull. 83 (2), 289–316.
- Long, D.J., Baco, A.R., 2014. Rapid change with depth in megabenthic structure-forming communities of the Makapu'u deep-sea coral bed. Deep Sea Res. Pt. II 99, 158–168.
- Macdonald, G.A., Abbott, A.T., Peterson, F.L., 1970. Volcanoes in the Sea. University Press of Hawaii, Honolulu.
- Coral reef ecosystems of the Northwestern Hawaiian Islands: interim results emphasizing the 2000 surveys. U.S. Fish and Wildlife Service and the Hawaii Department of Land and Natural Resources. In: Maragos, J.E., Gulko, D. (Eds.), 2002, Honolulu, Hawaii, 46.
- McClain, C.R., 2007. Seamounts: identity crisis or split personality? J. Biogeogr. 34 (12), 2001–2008.
- McClain, C., Lundsten, L., Barry, J., DeVogelaere, A., 2010. Assemblage structure, but not diversity or density, change with depth on a northeast Pacific seamount. Mar. Ecol. 31, 14–25.
- Mejía-Mercado, B.E., Mundy, B., Baco, A.R., 2019. Variation in the structure of the deepsea fish assemblages on necker island, northwestern Hawaiian islands. Deep Sea Res. Pt. I 152, 103086.
- Mejía-Mercado, B.E., Baco, A.R., 2022. Characterization and spatial variation of the deep-sea fish assemblages on Pioneer Bank, Northwestern Hawaiian Islands. Mar. Ecol. Prog. Series 692, 99–118. https://doi.org/10.3354/meps14071.
- Merrett, N.R., Haedrich, R.L., 1997. Deep-sea Demersal Fish and Fisheries, , first ed.vol. 23. Chapman & Hall, p. 287.
- Miller, J.E., Hoeke, R.K., Appelgate, T.B., Johnson, P.J., Smith, J., Bevacqua, S., 2003.
 Atlas of the Northwestern Hawaiian Islands (draft-February 2004). National Oceanic and Atmospheric Administration 65.
- Milligan, R.J., Morris, K.J., Bett, B.J., Durden, J.M., Jones, D.O.B., Robert, K., Ruhl, H.A., Bailey, D.M., 2016. High resolution study of the spatial distributions of abyssal fishes by autonomous underwater vehicle. Sci. Rep. 6, 26095.
- Milligan, R.J., Scott, E.M., Jones, D.O., Bett, B.J., Jamieson, A.J., O'brien, R., Pereira Costa, S., Rowe, G.T., Ruhl, H.A., Smith Jr., K.L., De Susanne, P., 2020. Evidence for seasonal cycles in deep-sea fish abundances: a great migration in the deep SE Atlantic? J. Anim. Ecol. 89 (7), 1593–1603.
- Morato, T., Clark, M.R., 2007. Seamount fishes: ecology and life histories. In: Seamounts: Ecology, Fisheries, and Conservation. Blackwell Publishing. Fish Aqua. Res. Ser, vol. 12, pp. 170–188.
- Morgan, N.B., Goode, S., Roark, E.B., Baco, A.R., 2019. Fine scale megafaunal assemblage structure of benthic invertebrates on the North Pacific seamount Mokumanamana. Front. Mar. Sci. 6, 715.
- Mortensen, P.B., Buhl-Mortensen, L., 2004. Distribution of deep-water gorgonian corals in relation to benthic habitat features in the Northeast Channel (Atlantic Canada). Mar. Biol. 144 (6), 1223–1238.
- Mundy, B.C., 2005. Checklist of the fishes of the Hawaiian archipelago. Bishop Mus. Bull. Zool. $6,\,1-704.$
- Nafpaktitis, B.G., 1977. Fishes of the western north Atlantic. Family neoscopelidae. Sears foundation for marine research. Memoir 1 (7), 1–12.
- NDSF (National Deep Submergence Facility), 2019. https://ndsf.whoi.edu/sentry/. Nelson, J.S., Grande, T.C., Wilson, M.V., 2016. Fishes of the World, fifth ed. John Wiley & Sons, New Jersey.
- Neter, J., Kutner, M.H., Nachtsheim, C.J., Wasserman, W., 1996. Applied Linear Statistical Models. Irwin, Chicago, Illinois, USA.
- NOAA (National Oceanic and Atmospheric Administration), 2003. Atlas of the Shallow-Water Benthic Habitats of the Northwestern Hawaiian Islands.
- NOAA (National Oceanic and Atmospheric Administration), 2019a. Gridded bathymetry of necker island, Hawaii, USA. Digital data extracted from. http://www.soest.hawa ii.edu/pibhmc/cms/data-by-location/northwest-hawaiian-islands/necker-island/ba thymetry/.
- NOAA (National Oceanic and Atmospheric Administration), 2019b. Gridded bathymetry of Pioneer Bank, Hawaii, USA. Digital data extracted from. http://www.soest.hawaii .edu/pibhmc/cms/data-by-location/northwest-hawaiian-islands/submerged-ban
- NOAA (National Oceanic and Atmospheric Administration), 2019c. Gridded bathymetry of French frigate shoals, Hawaii, USA. Digital data extracted from. http://www.soest.hawaii.edu/pibhmc/cms/data-by-location/northwest-hawaiian-islands/french-frigate-shoals/.

- Oksanen, J., Blanchet, F.G., Kindt, R., Legendre, P., O'Hara, R.B., Simpson, G.L., Solymos, P., Stevens, M.H.H., Wagner, H., 2010. Vegan: community ecology package. R package version 1.17-5. https://cran.r-project.org/web/packages/vega
- Oyafuso, Z.S., Drazen, J.C., Moore, C.H., Franklin, E.C., 2017. Habitat-based species distribution modelling of the Hawaiian deepwater snapper-grouper complex. Fish. Res. 195. 19–27.
- Parin, N.V., 1991. Fish fauna of the Nazca and Sala y Gomez submarine ridges, the easternmost outpost of the Indo-West Pacific zoogeographic region. Bull. Mar. Sci. 49 (3), 671–683.
- Parin, N.V., Mironov, A.N., Nesis, K.N., 1997. Biology of the Nazca and Sala y Gomez submarine ridges, an outpost of the Indo-West Pacific fauna in the eastern Pacific Ocean: composition and distribution of the fauna, its communities and history. Adv. Mar. Biol. 32, 145–242.
- Parrish, F.A., Baco, A.R., 2007. State of deep coral ecosystems in the US pacific islands region: Hawaii and the US pacific territories. In: Lumsden, S.E., Hourigan, T.F., Bruckner, A.W., Dorr, G. (Eds.), The State of Deep Coral Ecosystems of the United States. NOAA Technical Memorandum CRCP-3. Silver Spring MD.
- Parrish, F.A., Polovina, J.J., 1994. Habitat thresholds and bottlenecks in production of the spiny lobster (*Panulirus marginatus*) in the Northwestern Hawaiian Islands. Bull. Mar. Sci. 54 (1), 151–163.
- Polovina, J.J., Mitchum, G.T., Evans, G.T., 1995. Decadal and basin-scale variation in mixed layer depth and the impact on biological production in the Central and North Pacific, 1960-88. Deep Sea Res. Pt. I 42, 1701–1716.
- Powell, S.M., Haedrich, R.L., Mceachran, J.D., 2003. The deep-sea demersal fish fauna of the northern Gulf of Mexico. J. Northwest Atl. Fish. Sci. 31, 19–33.
- Priede, I.G., Godbold, J.A., King, N.J., Collins, M.A., Bailey, D.M., Gordon, J.D., 2010. Deep-sea demersal fish species richness in the Porcupine Seabight, NE Atlantic Ocean: global and regional patterns. Mar. Ecol. 31 (1), 247–260.
- Priede, I.G., 2017. Deep-sea Fishes: Biology, Diversity, Ecology and Fisheries. Cambridge University Press.
- Qiu, B., Koh, D.A., Lumpkin, C., Flament, P., 1997. Existence and formation mechanism of the North Hawaiian Ridge Current. J. Phys. Oceanogr. 27 (3), 431–444.
- Randall, D.J., Farrell, A.P., 1997. Deep-sea Fishes. Academic Press.
- Randall, J.E., 2007. Reef and shore fishes of the Hawaiian Islands. In: Sea Grant College Program. Univ. Hawai'i, Honolulu, p. 546.
- R Development Core Team, 2018. R: a language and environment for statistical computing. R Found. Stat. Comput. Vienna, Austria http://www.R-project.org.
- Reid, S.B., Hirota, J., Young, R.E., Hallacher, L.E., 1991. Mesopelagic-boundary community in Hawaii: micronekton at the interface between neritic and oceanic ecosystems. Mar. Biol. 109 (3), 427–440.
- Rex, M., 1981. Community structure in the deep-sea benthos. Annu. Rev. Ecol. Evol. Syst. 12 (1), 331–353.
- Rex, M.A., Etter, R.J., 2010. Deep-sea Biodiversity: Pattern and Scale. Harvard University Press, London, p. 354.
- Rex, M.A., Stuart, C.T., Hessler, R.R., Allen, J.A., Sanders, H.L., Wilson, G.D., 1993. Global-scale latitudinal patterns of species diversity in the deep-sea benthos. Nature 365 (6447), 636–639.
- Richer de Forges, B., Koslow, J.A., Poore, G.C.B., 2000. Diversity and endemism of the benthic seamount fauna in the southwest Pacific. Nature 405 (6789), 944.
- Rogers, A.D., 1994. The biology of seamounts. In: Blaxter, J.H.S., Southward, A.J. (Eds.), Ad Vances in Marine Biology, vol. 30. Academic Press, San Diego, CA, pp. 305–350.
- Rohde, K., 1992. Latitudinal gradients in species diversity: the search for the primary cause. Oikos 514–527.
- Rowden, A.A., Dower, J.F., Schlacher, T.A., Consalvey, M., Clark, M.R., 2010. Paradigms in seamount ecology: fact, fiction and future. Mar. Ecol. 31 (s1), 226–241.
- Samadi, S., Bottan, L., Macpherson, E., Richer De Forges, B., Boisselier, M.C., 2006. Seamount endemism questioned by the geographic distribution and population genetic structure of marine invertebrates. Mar. Biol. 149 (6), 1463–1475.
- Schlacher, T.A., Baco, A.R., Rowden, A.A., O'Hara, T.D., Clark, M.R., Kelley, C., Dower, J.F., 2014. Seamount benthos in a cobalt-rich crust region of the central Pacific: conservation challenges for future seabed mining. Divers. Distrib. 20, 491–502.
- Simons, R.A., 2011. ERDDAP—The environmental research Division's data access program. Available at: http://coastwatch.pfeg.noaa.gov/erddap.
- Snelgrove, P.V.R., Haedrich, R.L., 1985. Structure of the deep demersal fish fauna off Newfoundland. Mar. Ecol. Prog. Ser. 27 (1–2), 99–107.
- Somerton, D., Ianelli, J., Walsh, S., Smith, S., Godø, O.R., Ramm, D., 1999. Incorporating experimentally derived estimates of survey trawl efficiency into the stock assessment process: a discussion. ICES J. Mar. Sci. 56 (3), 299–302.
- Staudigel, H., Clague, D.A., 2010. The geological history of deep-sea volcanoes: biosphere, hydrosphere, and lithosphere interactions. Oceanography 23 (1), 58–71.
- Stein, D.L., Tissot, B.N., Hixon, M.A., Barss, W.H., 1992. Fish-habitat Associations on a Deep Reef at the Edge of the Oregon Continental Shelf. Fish. Bull. vol. 90, 540–551. Washington, D.C.
- Struhsaker, P., 1973. A Contribution to the Systematics and Ecology of Hawaiian Bathyal Fishes. PhD dissertation, the University of Hawaii at Manoa, Honolulu.
- Suess, E., 1980. Particulate organic carbon flux in the oceans-surface productivity and oxygen utilization. Nature 288 (5788), 260–263.
- Thistle, D., 2003. The deep-sea floor: an overview. In: Tyler, P.A. (Ed.), Ecosystems of the World. Elsevier, New York, pp. 1–37.
- Tolimieri, N., Clarke, M.E., Singh, H., Goldfinger, C., 2008. Evaluating the SeaBED AUV for monitoring groundfish in untrawlable habitat. In: Reynolds, J.R., Greene, H.G. (Eds.), Marine Habitat Mapping Technology for Alaska. Alaska Sea Grant College Program. Univ. of Alaska Fairbanks, pp. 129–141.

- Tracey, D.M., Bull, B., Clark, M.R., Mackay, K.A., 2004. Fish species composition on seamounts and adjacent slope in New Zealand waters. New Zeal. J. Mar. Fresh 38 (1), 163–182.
- Tracey, D.M., Clark, M.R., Anderson, O.F., Kim, S.W., 2012. Deep-sea fish distribution varies between seamounts: results from a seamount complex off New Zealand. PLoS One 7 (6), e36897, 1–12.
- Uchida, R.N., Uchiyama, J.H., 1986. Fishery atlas of the northwestern Hawaiian islands. NOAA (Natl. Ocean. Atmos. Adm.) Tech. Rep. NMFS (Natl. Mar. Fish. Serv.) 38.
- Vroom, P.S., Page, K.N., Peyton, K.A., Kukea-Shultz, J.K., 2006. Marine algae of French Frigate Shoals, Northwestern Hawaiian Islands: species list and biogeographic comparisons. Pac. Sci. 60 (1), 81–95.
- Weiss, J., Miller, J., Hirsch, E., Rooney, J., Wedding, L., Friedlander, A., 2009. Geology and benthic habitats. In: Friedlander, A., Keller, K., Wedding, L., Clarke, A., Monaco, M. (Eds.), A Marine Biogeographic Assessment of the Northwestern Hawaiian Islands. NOAA Technical Memorandum NOS NCCOS 84. Prepared by NCCOS's Biogeography Branch in Cooperation with the Office of National Marine Sanctuaries Papahānaumokuākea Marine National Monument. Silver Spring, MD, p. 363.
- White, M., Bashmachnikov, I., Aristegui, J., Martins, A., 2007. Physical processes and seamount productivity. In: Pitcher, T.J., Morato, T., Hart, P.J.B., Clark, M.R., Haggan, N., Santos, R.S. (Eds.), Seamounts: Ecology, Fisheries, and Conservation. Fish and Aquatic Resources Series 12. Blackwell Publishing, Oxford, UK, pp. 65–84.
- Wynn, R.B., Huvenne, V.A., Le Bas, T.P., Murton, B.J., Connelly, D.P., Bett, B.J., Ruhl, H. A., Morris, K.J., Peakall, J., Parsons, D.R., Summer, E.J., Darby, S.E., Dorrell, R.M., Hunt, J.E., 2014. Autonomous Underwater Vehicles (AUVs): their past, present and future contributions to the advancement of marine geoscience. Mar. Geol. 352, 451–468.
- Wishner, K., Levin, L., Gowing, M., Mullineaux, L., 1990. Involvement of the oxygen minimum in benthic zonation on a deep seamount. Nature 346 (6279), 57–59.
- Wren, J.L., Kobayashi, D.R., Jia, Y., Toonen, R.J., 2016. Modeled population connectivity across the Hawaiian archipelago. PLoS One 11 (12), e0167626.
- Yeh, J., Drazen, J.C., 2009. Depth zonation and bathymetric trends of deep-sea megafaunal scavengers of the Hawaiian Islands. Deep Sea Res. Pt. I (56), 251–266.
- Zimmermann, M., 2003. Calculation of untrawlable areas within the boundaries of a bottom trawl survey. Can. J. Fish. Aquat. Sci. 60 (6), 657–669.
- Zuur, A.F., Ieno, E.N., Elphick, C.S., 2010. A protocol for data exploration to avoid common statistical problems. Methods Ecol. Evol. 1 (1), 3–14.